Switching to the Brighter Lane: Pathways to Boost the Absorptionof Lanthanide-Doped Nanoparticles

Riccardo Marin,[1] Daniel Jaque [1] and Antonio Benayas[1]

[1] Fluorescence Imaging Group, Departamento de Física de Materiales – Facultad de Ciencias, Universidad Autónoma de Madrid, C/Francisco Tomás y Valiente 7, Madrid 28049, Spain

E-mail: riccardo.marin@uam.es

Switching to the Brighter Lane: Pathways to Boost the Absorptionof Lanthanide-Doped Nanoparticles

1. Introduction

Despite suggestions of turning the periodic table upside down,[1] lanthanides (from the Greek word *lanthaneien* meaning ''lyinghidden'') continue to occupy the bottom part of it together with their bigger brothers, the actinides. This representation makeslanthanides quite literally "outstanding" elements not only fortheir unique properties. Lanthanides, which along with scandium and yttrium form the family of rare earths, are indeed elements of strategic interest for several applications. Anti- counterfeiting tags in banknotes, blue-light conversion layer in LEDs, permanent magnets, and lighter flints are some of the mundane objects through which we cross path with lanthanides on a daily basis. Other materials are more exotic, such as lanthanide complexes behaving as magnets at the single-molecule level (single-molecule magnets - SMMs).[2, 3] But whatwe are interested in here is a particular family of materials thatcapitalize on the light emitted by trivalent lanthanide ions (Ln^{3+}): colloidal nanoparticles doped with Ln^{3+} (LNPs). LNPs arethe workhorses in several fields of nanotechnology owing to their capability, for example, to act as optical probes[4-6] and photo initiate chemical reactions under excitation with low- energy photons.[7, 8] The small size of LNPs makes them usable in microenvironments (e.g., cells),[9] and more generally for the investigation of phenomena with sub-micrometric accuracy while minimally perturbing the observed system.[10, 11] They have also been proposed for the preparation of light harvesting layers for low-energy photons, which would otherwise go unexploited in photovoltaic devices.[12, 13] All in all, LNPs deservedly gained a place of respect in the field of nanotechnology alongside their older kin featuringphotoluminescence properties: the family of semiconductor nanocrystals. LNPs and semiconductor nanocrystals are both inorganic luminescent nanoparticles. However, the similaritiesbetween them end there. Numerous discrepancies exist in terms of chemistry and physics, hence making each of these nanomaterials suited for specific applications where the othermight need to stretch. Hence, LNPs and semiconductor nanocrystals are complementary rather than competing, both with their advantages and shortcomings. Speaking of the latter, LNPs' most notable limitation resides in their low overall emission intensity, which is a result of the electron configuration of Ln^{3+} ions (*vide infra*). This poor emission *brightness* (which we more rigorously define further below) represents the major bottleneck to the widespread employment of LNPs in fields like lighting and optical imaging.But brighter LNPs would also translate to better performance in applications where these species are already routinely employed, like in the field of sensing.

In this Review, we discuss the recent advances in the development of brightly emitting LNPs. In Section 2, we present in simple and comprehensive terms the "brightness issue" thataffect Ln^{3+} luminescence. We then proceed in Section 3 to critically review the methods developed so far for tackling thisissue. Although several approaches have been proposed, we herein focus on three specifically: use of plasmonic moieties toincrease the absorption (and emission) prowess of Ln^{3+}, and sensitization of Ln^{3+} emission through the use of organic dyes and semiconductors. Lastly, in Section 4 we provide an overview of the field, suggesting the still unresolved questions, also identifying the most promising and probable research directions.

2. Lanthanide ions and their forbidden transitions

Trivalent lanthanides (Ln^{3+}) owe most of their properties to non- bonding electrons occupying the 4f orbitals. Precisely becauseof this lack of involvement of 4f electrons in the formation of bonds, at the single-ion level Ln^{3+} feature remarkably similar physical properties *in vacuo* and when bound to other elements to form compounds. The "ladder" of 4f electronic states of each Ln^{3+} (**Figure 1**) is in fact screened by external charge densities from the 5s and 5p orbitals. Thus, the electrons can jump undisturbed between the steps of the 4f ladder, but they should obey to an important quantomechanical constraint: the parity(Laporte) rule.[14] This rule states the impossibility of electronic transitions between states with the same parity (such as 4f-4f intraconfigurational transitions) to occur in centrosymmetric environments. Fortunately, even when a Ln^{3+} is placed in the centre of a perfectly centrosymmetric coordination polyhedron, f-f electronic transitions can still occur thanks to vibration that induce a temporary reduction of the symmetry. Moreover, admixing with opposite/parity wavefunctions (e.g., 5d orbitals and/or

coordinating ligands) can also cause the breakdown ofthis selection rule. Of course, the forbidden nature of these transitions decreases the probability of an electron to be excited to a higher-energy state as well as relax to a less energetic one. Therefore, when (and if) and electron is promoted by the absorption of a photon to a higher step of theladder, it will sit there for a relatively long time (micro- to milliseconds) before being kicked up to an even more energetic state or relaxing to a lower lying one. In the right conditions, such relaxation is accompanied by the release of energy in theform of a photon, whose energy matches the energy difference between initial and final states, rather than as heat generatedby vibrations. Overall, the unique electronic configuration of Ln^{3+} results in emissions that are narrow (atom-like), fall at relatively constant energies (changing by few hundreds of cm^{-1}at most), and have extended lifetimes. The long-lived nature of4f electronic states is desirable since it can be harnessed to generate the non-linear optical phenomenon of upconversion(UC). This process entails the sequential absorption of multiple low-energy photons followed by radiative relaxation of the excited electron with the emission of a single higher-energy photon.[15]

However, the reduced probability of those transitions also translates to poor light absorption. From an optical standpoint,this is the more relevant shortcoming of Ln^{3+} ions since it limitsthe effectiveness of direct excitation of 4f electrons responsible for the emission. Quantitatively, the capability to absorb a photon of specific energy (i.e., wavelength) is defined by the molar extinction coefficient, expressed in units of length per mole. This parameter is in the order of 0.1-10 $M^{-1}cm^{-1}$ for Ln^{3+},while semiconductor nanocrystals and organic dyes feature much larger values in the 10^4-10^6 $M^{-1}cm^{-1}$ range. The product of this parameter and the photoluminescence quantum yield (PLQY - # emitted photons per # absorbed photons) gives the brightness of a species. This is arguably the most important parameter to consider for practical uses, as it provides an estimation of how much of the excitation light shined on the luminescent species will eventually be converted to emitted light. However, not all Ln^{3+} are the same. Some, like Nd^{3+} and Yb^{3+}, can absorb light more effectively than others and are thusused as *sensitizers*, i.e., ions that absorb the excitation light and transfer this energy to the emitting ion (*activator*). Use of sensitizer-activator pairs is at the basis of the preparation of LNPwith good emission brightness. However, more sophisticated strategies have been developed to improve on this concept. In the next section, we discuss selected approaches for the enhancement of this parameter in nanoparticles doped with Ln^{3+} ions, which aim at increasing the excitation light absorption capability of the nanostructure.

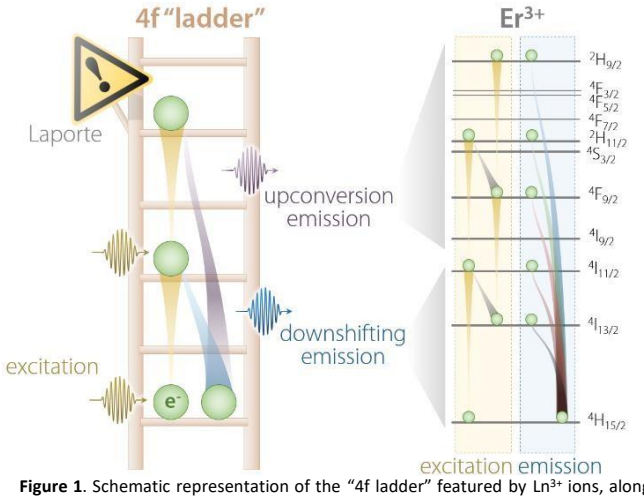

Figure 1. Schematic representation of the "4f ladder" featured by Ln^{3+} ions, along with the real example of Er^{3+} excitation and emission processes under 980-nm excitation.

3. Strategies to enhance the brightness of Ln^{3+}nanophosphors

Several researchers have been working on the optimization ofLNP-based nanosystems with the goal of maximising the amount of light absorbed and the fraction of energy funnelledto the activator ion (**Figure 2**). This effort resulted in several approaches. Some of them entail the introduction of lattice distortion-inducing ions[16-18] and preparation of multi-shell structures.[19-21] The former approach aims to manipulate the crystal field experienced by the Ln^{3+} ion, increasing the f-f electronic transition probabilities by partial admixing of 4f wavefunctions with opposite-parity ones (i.e., 5d orbitals). Thelatter approach is instead underpinned by concepts such as maximization of sensitizer concentration, spatial segregation of ions, and surface passivation of the LNP. These approaches push the limit of the

intrinsic optical properties of Ln^{3+} and are not discussed in the present Review – the interested reader is encouraged to read the above cited works. Another strategy entails co-doping of Ln^{3+} with ions featuring allowed electronic transitions, such as Ce^{3+},[22, 23] Bi^{3+},[24] and $Mn^{3+/4+}$,[25] which can more effectively absorb light and transfer it to nearby activators (**Figure 2**). These ions can also introduce additional energy levels that act as intermediate states for the population of Ln^{3+}, increasing the energy transfer efficiency and enabling fine tuning of the emission colour. In this Review, we do not examine these approaches either. In the following sections, we focus our attention on three strategies. One of them acts via enhancement of the absorption (and emission) probability of the Ln^{3+}-doped material per se: the use of plasmonic nanostructures. The other two rely on light harvesting moieties of different nature: organic dyes, and semiconductor nanocrystals (SNCs). For each strategy, we outline the general principle at its basis, passing then to the description of the involved physical processes and listing of the requirements to be met to successfully prepare a brightly emitting colloidal LNP following the selected strategy.

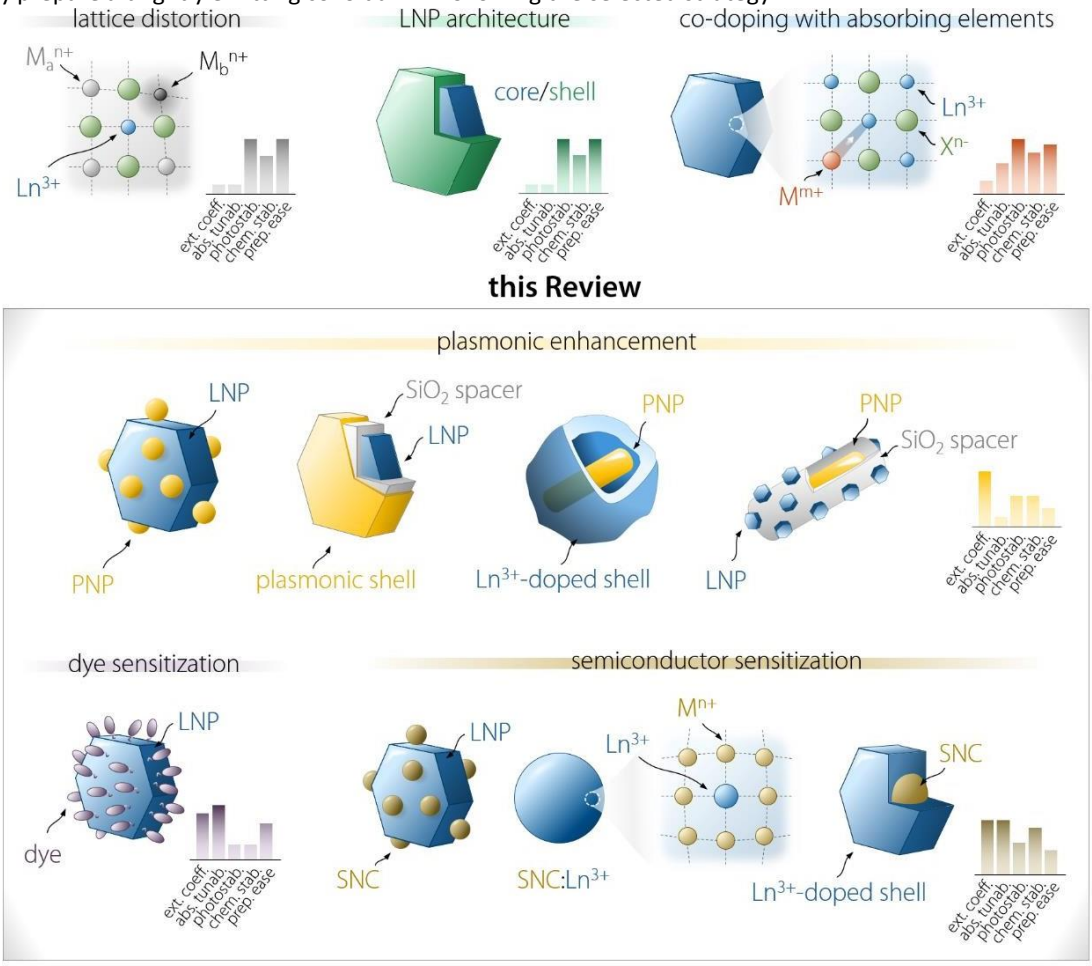

Figure 2. Graphical summary of the strategies employed for the enhancement of Ln^{3+} emission brightness. The modification of the lattice by incorporation of defects and lattice- distorting ions effectively lowers the coordination symmetry of the Ln^{3+}, ultimately leading to a relaxation of the parity rule for intraconfigurational f-f transitions. Preparation of LNPs with multi-shell architecture, where different Ln^{3+} ions are spatially confined and protected from quenchers (e.g., solvent molecules with high-energy vibrations) allows minimizing energy losses, thus yielding brighter Ln^{3+} emission. Co-doping with Ln^{3+} and ions featuring allowed electronic transitions (Ce^{3+}, Bi^{3+}…) is a viable strategy to enhance the light absorbing capability of LNPs. Those approaches, albeit being of relatively easy realization, theoretically afford a limited enhancement of the LNP capability to absorb excitation light. For this reason, in this Review we focus on three other approaches which can theoretically grant more efficient sensitization (i.e., excitation light absorption followed by energy transfer to the emitting ion) of Ln^{3+} luminescence. Plasmon-enhancement entails the use of moieties featuring localized surface plasmon resonance (LSPR), which can improve both absorption and emission efficiency of the coupled LNP. Dyes and semiconductors can both be used as excitation light harvesters and, upon proper coupling/amalgamation with LNPs, they can transfer the absorbed energy to the Ln^{3+}. These latter strategies promise the highest absorption betterment and tunability, but the synthesis of those nanosystems require a higher degree of finesse.

3.1. Plasmonic enhancement

Among the alternatives discussed in this Review, the use of plasmonic materials is by far the most explored pathway

for the enhancement of LNPs' emission. A plasmon is a quasiparticle that defines the collective motion of free charge carriers withina conductor material (such as metals), which occurs at a frequency characteristic of the material itself. Surface plasmon(polaritons) resonances (SPR) result from the hybridization of bulk plasmons with free-space radiation, which takes place at the interface of the plasmonic material and a dielectric medium. Along with the nature of the conducting material, the dielectric constant of the medium determines the oscillation frequency of the charge carriers. When the carriers are spatially confined, as it is the case for a plasmonic nanoparticle (PNP), the natural frequency of these collective charge also depends on the size and geometry of the PNP. This is referred to as localized surface plasmon resonance (LSPR) and is the phenomenon of interest in the current frame. In fact, although numerous are the examples of (UC) emission enhancement using patterned plasmonic surfaces and 2D structures,[26, 27] we are herein focusing only oncolloidal systems. Clearly, for preparing such systems, PNPs ought to be used.

The enhancement of Ln^{3+} emission stems from the influence ofsurface plasmons on three distinct parameters, which synergistically contribute to determining the overall emission brightness: decay rates (i.e., radiative and non-radiative relaxations), energy transfer coefficients and absorption crosssection.[28] We should note here that albeit the focus of this Review is the betterment of the absorption capability of LNPs,to comprehensively address the topic plasmon-enhanced emission we discuss also cases wherein the radiative decay rate is playing a major role. Indeed, often the effects cannot be completely disentangled and other times the explanation offered by the authors for the observed emission enhancement is more an "educated guess" than a definitive explanation. An in-depth discussion of the fundamentals of each aspect lies beyond the scope of this manuscript, and the interested readeris encouraged to read the instructive review from Park et al.[28] For the sake of the present discussion, it is sufficient to say that

i) absorption is mainly influenced by local field enhancement, ii) radiative decay rate is enhanced by an increased photon density of states (Purcell effect), iii) non-radiative relaxation is impacted by ohmic losses induced by the presence of metal, iv) experimental reports indicate that energy transfer enhancement is generally observed for systems with large donor-acceptor separation distance – and as such featuring intrinsically inefficient transfer. Regarding the last point, in thecase of LNPs the donor-acceptor distance refers to the separation between sensitizer and activator ions in the particlelattice. Considering the large amount of sensitizers introducedin LNPs (often between 20 and ~100%)[29], the average distancebetween neighbouring ions is short, making the energy transfer between them efficient enough so that its further enhancement using plasmonic moieties is difficult to achieve.[30] Importantly, the interplay between the first three points yields an emissionenhancement factor whose maximum falls at a specific separating distance between the LNP and PNP.[31] This distancedefines the optimal thickness of the spacer between the two moieties (**Figure 3A** – generally in the order of 10 to few tens of nanometres). In the case of LNP-PNP coupling, such spacer is often made of silica,[31-35] but polymers have also been used[36, 37]. Another important aspect to consider is that larger PNPs always feature stronger scattering of light, which induce higher luminescence enhancement compared to their smaller counterpart.[38, 39] Smaller particles whose LSPR peak overlaps with the emission support instead a more efficient quenching of the luminescence via energy transfer (likely due to their dominant absorption over scattering).[40] This is a pivotal consideration, which provides further guidelines for the design of the most suitable plasmonic system for plasmon-enhanced luminescence.

Considering the observations above, the enhancement of LNPemission can be achieved matching the excitation and/or the emission wavelengths – exploiting the absorption enhancement and the radiative decay rate increase, respectively (**Figure3B**).[41, 42] This was demonstrated also in dye molecules coupledto individual silver nanoprisms.[43] Regarding LNPs in particular,it is important to note that while plasmon-induced enhancement of downshifting emission has a quadratic dependence on the local field enhancement, the anti-Stokes process of UC depends on the fourth power of this parameter.[28, 44] It comes as no surprise then that studies on plasmon- enhanced UC are far more common than studies on downshifting enhancement; also because emission processes that are intrinsically poorly efficient (like UC) are more easily enhanced harnessing plasmonic effects. Nonetheless, we should point out that UC is a process that relies on the long-livednature of Ln^{3+} energy states for successive absorption of photons. Therefore, any increase of the decay rate of an intermediate energy state involved in the population of higher- energy levels is detrimental to this non-linear optical process. A fitting example is offered by an Yb^{3+}-Er^{3+} co-doped material, where excitation of Yb^{3+} at 980 nm fosters UC emission of Er^{3+}.In several instances it was observed that a perfect matchbetween LSPR and Yb^{3+} absorption was not the most favourable situation for plasmon-enhancement.[45] A wavelength mismatchallowed instead maximising the optical performance of the combined system, likely due to a less pronounced lifetime shortening (i.e. decay rate increase) of Yb^{3+} $^4F_{5/2}$ excited level -happening in particular for zero-phonon transitions. Lastly, a point should be made regarding the versatility of plasmon enhancement as a strategy. The position of the

LSPR peak featured by PNPs can be controlled by several means: nature of the plasmonic material, size and morphology, as wellas presence of interfaces with different materials are all parameters which can be harnessed to fine-tune the LSPR position. Gold is the most versatile material for the preparation of PNPs and decades of experience have produced a vastliterature of synthetic approaches. Nanospheres, nanorods(GNRs), nanoshells (GNSs), and nanourchins are only some of the proposed gold-based PNPs, and their LSPR covers a wide gamut of wavelengths, form visible to the second biological window (NIR-II, 1000-1350 nm). Silver is another noble metal with suitable plasmonic properties, but also some oxides (indium tin oxide - ITO,[46] W_xO[47]), chalcogenides (Cu_xS, Cu_xSe)[48],and borides (LaB_6)[49] nanoparticles feature LSPR. For many of these latter PNPs, the plasmonic resonance can easily be extended in the near-infrared (NIR) beyond 1000 nm, whereasPNPs based on noble metals tend to have their LSPR in the visible (unless cumbersome or high-aspect-ratio systems are prepared). Despite this flexibility, coupling of PNP with LNP does not afford broadband excitability. Indeed, the excitation wavelength is still determined by the Ln^{3+} whose absorption isto be enhanced.

In the rest of this section we discuss selected examples of plasmonic enhancement of LNP emission, subdividing the approaches depending on the architecture of the final system.As mentioned above, the almost totality of the examples dealwith UCNPs.

Decoration with of LNP with PNPs. One of the most straightforward approaches explored for the plasmonic manipulation of LNP's emission is their decoration with PNPs. This method is generally accomplished with gold and silver NPs, whose LSPR peak falls predominantly in the visible part of the electromagnetic spectrum. This enables harnessing the Purcelleffect to enhance the UC emission.[50] However, above 100 nm in size, the extinction spectrum of gold NPs extends more decisively in the NIR. In that vein, it was observed by Fischer etal. that larger gold NPs are better suited to enhance Er^{3+} emission at 980 nm under 1520-nm excitation, due to increased scattering of large structures.[38] When it comes to colloidal systems, both enhancement and quenching of the emission were observed in LNPs decorated with PNPs. To that end, silver PNPs (λ_{LSPR} = 415 nm) were used to enhance the emission of $NaYF_4$:Nd^{3+},Yb^{3+},Ho^{3+} LNPs.[52] The authors found that a 10-nm thick SiO_2 spacing layer afforded the largest enhancement factors (15 and 7.5 for green and red emission respectively) both under 808 and 980-nm excitation in cyclohexane. The enhancement there followed from the increase of the emission decay rate (Purcell effect) rather than from absorption enhancement – as expected also from the lack of overlap between LSPR and excitation light. These results were consistent with those obtained for $NaYF_4$:Yb^{3+},Er^{3+} LNPs combined with 15-nm silver PNPs.[35] Duan, Huang and co- workers compared the effect of sub-micrometric LNP decoration with gold PNPs and the growth of a continuous gold shell (**Figure 3C**).[51] LNPs were successively decorated with polyacrylic acid (PAA) and polyallylamine hydrochloride (PAH) exploiting the negative and positive charge respectively featured by the two polymers. Gold PNPs (seeds) were then attached to the surface of the LNPs (made of $NaYF_4$:Yb^{3+},Tm^{3+}), and their coalescencewas induced by addition of gold precursor in the suspension, yieldinga continuous metal shell. Enhancement of Tm^{3+} emission (452, 478, and 647 nm) was observed only in the presence of PNPs with absorption in the visible, while quenching was induced by the metal nanoshell. This last effect was ascribed to scatteringof the excitation light (owing to the NIR-centred LSPR of the shell), yielding a lower overall excitation light flux and to reduced transmission of the UC emission through the shell. Xing et al. prepared a sub-50 nm system comprising $Na(Y,Gd)F_4$:Yb^{3+},Er^{3+},Tm^{3+}/SiO_2/gold nanospheres.[53] Several UC emission lines stemming from Er^{3+} and Tm^{3+} were observed between 500 and 800 nm, while the gold PNPs featured an extinction stretching throughout the whole visible range. Upon optimization of the spacer thickness (10-15 nm) and PNPs amount, a 3/4-fold enhancement of the UC emission was achieved. The brighter luminescence allowed for *in vitro* and *in vivo* visualization of the particles under 980-nm excitation, while the magnetic and X-ray absorption properties of Ln^{3+} also granted MRI and computed tomography imaging capabilities.Similarly, Jiang et al. demonstrated an almost 80-foldenhancement of Gd^{3+} UC emission in $NaYF_4$:Gd^{3+},Yb^{3+},Tm^{3+} upon fine control of the total amount of attached small gold PNPs.[54] One limitation of the approaches discussed above is that the spectral overlap between LSPR and LNP emission could also induce to absorption of the emitted light by the PNPs. This scenario is most detrimental for the increment of the brightness of LNPs, but it can be harnessed for bio-assays and for colour- tuning.[34, 55-58]

Betterment of the UC luminescence was observed also in GNR-decorated $NaYF_4$:Yb^{3+},Tm^{3+} LNPs.[36] Polyamidoamine dendrimer was used to functionalize the surface of LNPs, and GNRs weregrown in-situ on the surface of the structure. The extinction

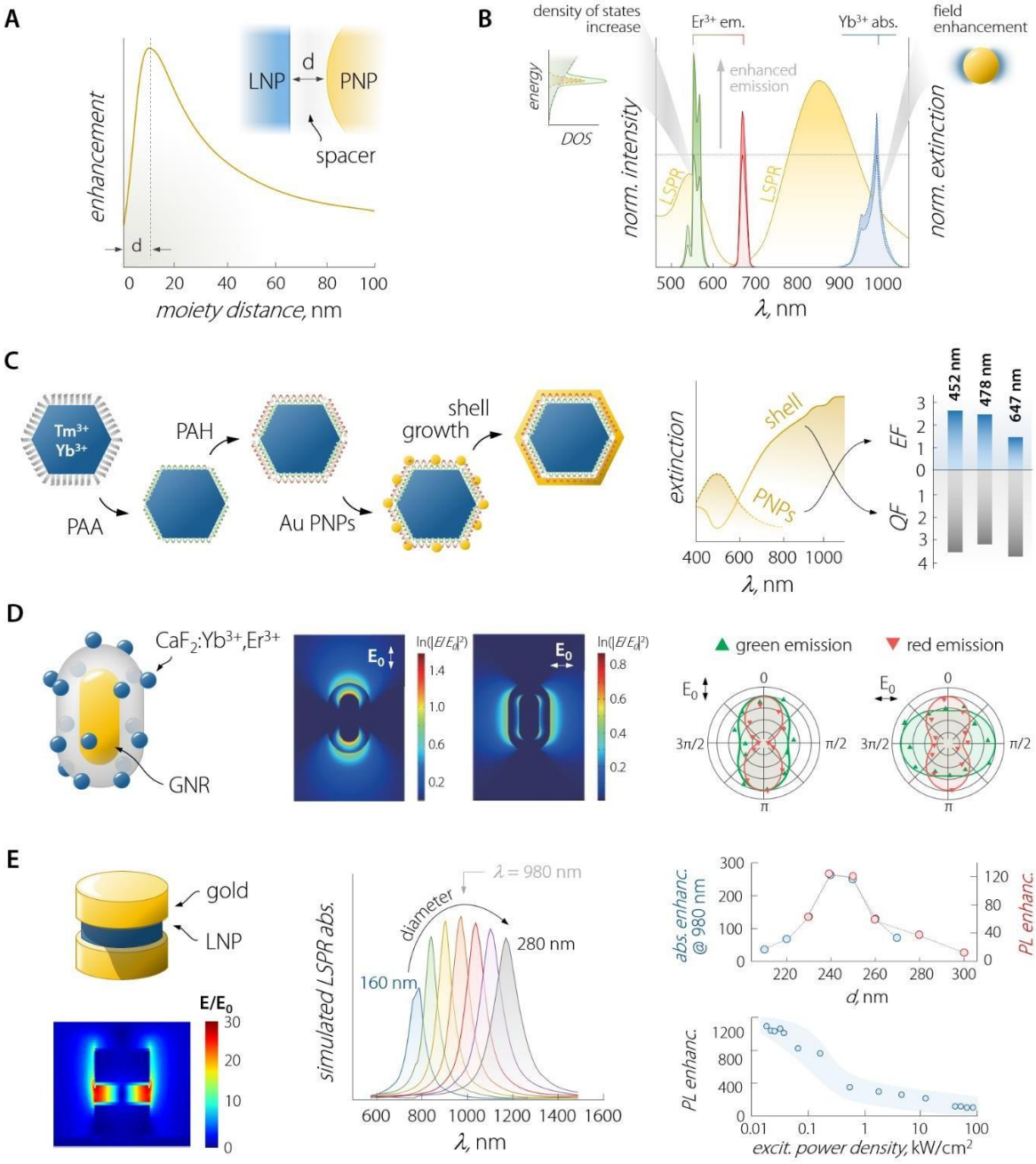

Figure 3. Plasmon-enhanced LNP emission. **A)** the enhancement factor is a complex function of the PNP-LNP separation distance with its maximum falling at a value determined by several effects discussed in the main text. **B)** plasmon-enhancement in a Yb^{3+}/Er^{3+} upconverting system, where absorption (due to local field enhancement) and emission (due to the Purcell effect) are simultaneously achieved. **C)** scheme of sequential decoration of Yb^{3+}/Tm^{3+}-doped LNP with gold nanospheres and complete coverage with gold nanoshell, along with the extinction spectra and enhancement/quenching factors observed for the two architectures. Adapted with permission from Ref. [51]. Copyright 2010 Wiley-VCH. **D)** Decoration of a single SiO_2-coated GNR with CaF_2-based small LNPs. The local field enhancement under 980-nm excitation varies sizeably in intensity and spatial distribution depending on the relative orientation of the impinging light (E_0) and the GNR. The different behaviour of the observed polarization of green and red emitted light arises mainly from the coupling between LSPR and UC emission, rather than from the laser polarization. Adapted with permission from Ref. [32]. Copyright 2016 Springer-Nature. **E)** In a structure comprised of LNPs

spectrum of GNRs was characterized by two contributions at 520 and 805 nm, owing to the transverse ad longitudinal modes respectively. Upon extending the GNR growth time to 240 min, the light extinction efficiency of the plasmonic particles increased, resulting in a maximum 27-fold enhancement of NIR- to-NIR UC luminescence (Tm^{3+} emission at 800 nm) under 980-nm excitation. At shorter growth times, the GNRs had a smalleraspect ratio, which resulted in preferential improvement of the UC visible emission (11.2-fold) compared to NIR. The nanocomposite (GNRs + LNP) functionalized with 2-thiouracil was employed by the authors for uric acid (UA) sensing: UA induced aggregation of the particles, yielding changes in both extinction and luminescence spectra. Both signals could be used to determine UA concentration with detection limit as low as 1pM.

Decoration of PNP with LNPs. In recent years, thisapproach has been extensively exploited by several researchers. The most common structure is a single (or a pair of[59]) high-aspect ratio PNP (such as a GNR) coated with a silicalayer of controlled thickness (spacer), on top of which several small LNPs are attached (**Figure 3D**).[32, 42, 60] Simultaneous excitation and emission enhancement was achieved by Kang etal. using engineered core/shell/shell LNP to decorate the surface of a 25x80 nm GNR coated with a 28-nm thick mesoporous SiO_2 layer.[42] The transverse LSPR was centred in the green region, while the longitudinal mode fell in the NIR, encompassing both 808 and 980 nm (i.e., the excitation wavelengths used for Nd^{3+} and Yb^{3+} excitation, respectively). Itis interesting to note that studies for plasmonic enhancement of LNP emission generally make use of rather simple LNP architectures, while in the mentioned study segregation of sensitizers (Nd^{3+}, Yb^{3+}) and activator (Er^{3+}) in different LNP regions, along with the growth of a passive shell were performed. Overall, an enhancement factor of 20 was achieved for green emission (upon 808-nm excitation), whose lifetime was substantially shortened due to the Purcell effect (and possibly to the introduction of other non-radiative decay pathways). A similar system was prepared by He et al., who employed CaF_2:Yb^{3+},Er^{3+} LNPs, which were tethered to the surface of SiO_2-coated GNRs (**Figure 3D**).[32] The authors observed enhanced green and red UC emission, owing to the spectral overlap of these emission lines with the transversal and longitudinal LSPR modes of the GNR. Even more interestingly, it was verified that the emitted light was strongly polarized. While the polarization of red emission did not show correlation with the relative orientation of the GNR axis and the polarization direction of the excitation light (E_0), green UC emission appeared to be dependent on that parameter. This behaviourstemmed from the stronger contribution to the overall emission coming from LNPs located at the tips or at the sides of the GNR when E_0 is, respectively, parallel or perpendicular to the GNR's axis. Indeed, while red UC emission remained polarized along the GNR axis irrespective of the excitation light orientation andLNP location, green UC emission polarization changed depending on those two parameters. By performing electrodynamic calculations within the frame of FRET theory, the authors could unravel the complex interactions underpinning this behaviour. In particular, the relative orientation and degree of interaction between emission dipoles in the LNPs and the transverse and longitudinal plasmonic dipoles within the GNR were shown to play a key role.

3.1.1. Growth of plasmonic shells on LNPs. Considering gold- based plasmonic nanostructures, an effective way to push their LSPR in the NIR (thus matching the absorption of typical Ln^{3+} used as sensitizers, like Nd^{3+} and Yb^{3+}) is the preparation of nanoshells. These are structures of few nanometres in thickness grown on top of a dielectric core, such as silica particles. Tuning of the ratio between SiO_2 core size and metal thickness allowscontrolling the position of the LSPR peak. SiO_2-coated LNPs covered with a layer of noble metal are indeed among the most explored structures in this context – although growth of a goldshell directly on LNP has been performed too. In this vein, we mentioned in Section 3.1.1 the study from Duan, Huang and co- workers, wherein a gold shell was grown atop of LNPs. Compared to decoration with PNPs, the observed effect of a gold shell was the quenching of $NaYF_4$:Yb^{3+},Tm^{3+} emission (**Figure 3C**).[51] However, successful enhancement of LNP emission was achieved in other studies. For instance, direct growth of a gold shell on citrate-functionalized cubic α- $NaYF_4$:Yb^{3+},Er^{3+} or Tm^{3+} NPs afforded UC emission intensity comparable to that exhibited by the same material in the hexagonal (β) polymorph.[61] Priyam et al. controlled the thickness of the gold shell grown on SiO_2-coated $NaYF_4$:Yb^{3+},Er^{3+} LNPs, effectively tuning the LSPR peak maximum from 580 to 900 nm.[62] The thinner the shell the more red-shifted the extinction. Enhancement was observed only in the case of 900-nm centred LSPR, thanks to the highest extinction at 980 nm (i.e., the LNP excitation wavelength) and reduced LSPR overlapwith Er^{3+} emission lines (centred at 410, 550 and 660 nm). All the other tested LNP/SiO_2/GNSs showed instead a quenched UC emission. The optimized nanostructure was used for simultaneous fluorescence and dark field imaging (leveraging the scattering of the GNS for the latter) of B16-F0 cells. Kannanet al. explored instead a silica-free approach, where the LNPs were modified with a polyamidoamine dendrimer of first generation (PMAM G1).[37] The polymer offered a suitable substrate over which gold or silver shells were grown, yielding respectively increased green and UV-blue UC emission enhancement.

3.1.2. Growth of Ln^{3+}-doped shells on PNPs. A strategy complementary to the one discussed above is the growth of aLn^{3+}-containing shell on a PNP. Different approaches have been explored, such as growth of the Ln^{3+}-doped shell directly on the surface of the plasmonic particle,[63] use of a spacer between the two species,[33, 64-66] as well as selective etching of the silica spacer to achieve rattle-like structures[65, 67]. Stucky and co- workers grew a Y_2O_3:Er^{3+} shell on SiO_2-coated silver NPs[65] adapting a strategy for the preparation of rare-earth nanostructures with urea and rare-earth salts.[68] Optimal spacer thickness was found to fall between 20 and 40 nm, dependingon the diameter of the silver NP (from 20 to 130 nm). An analogous structure was prepared replacing Ag NPs by Au NPs:an optimal spacer thickness of 40 nm afforded an almost 10-fold enhancement of green Er^{3+} emission thanks to the overlap of the LSPR peak (centred at 527 nm) with Er^{3+} emission.[66] A shellof Lu_2O_3:Gd^{3+},Yb^{3+},Er^{3+} was also grown on SiO_2-coated Ag NPs using the same approach.[64] The resulting nanosystem was used as a probe for fluorescence imaging of HeLa cells and featured a 30-fold enhancement of the luminescence compared to the control sample lacking PNP. Interestingly, similar structures with GNRs coated with Ln^{3+}-doped fluoride[69, 70] or oxyfluoride[71] shells showed a quenched UC emission. Recently, it was reported the first example of plasmonic-enhancement of the UC luminescence of colloidal LNPs using a non-metal-based PNPs. $Cu_{1.8}S$ nanoparticles were coated with two shells of $NaYF_4$ doped respectively with Yb^{3+} and Yb^{3+}-Er^{3+}.[72] The NIR-centred LSPR of the chalcogenide PNPs, along with optimization of the Yb^{3+} content in the intermediate layer (30%), afforded a maximum 40-fold enhancement of UC emission thanks to enhancement of the absorption capability of the system. Lastly, moving from UC, the enhancement of Nd^{3+} downshifting emission was achieved in GNR/Nd_2O_3 nanocomposites.[67] The structure was prepared via a hydrothermal method at relatively low temperature (85 °C) and tuning of the LSPR allowed reaching a maximum enhancement factor of approximately 4.6 for Nd^{3+} emission at 873 nm under 730-nm excitation.

Other structures. Aside from the appearance of extended polaritons in periodic structures, the reason why patterned surfaces are often used for the enhancement of the luminescence has to be searched in the non-isotropic nature of the electromagnetic field enhancement.[73] In fact, on surfaces it is possible to control the relative disposition and orientation ofthe plasmonic antennas and LNPs. Confinement of the enhanced field in selected regions and careful positioning of the LNPs therein affords unrivalled plasmon-mediated sensitization. Clearly, control over the relative spatial orientation of LNP and PNP is pivotal also in a colloidal system.Unfortunately, this directionality is not easily achieved with classical wet chemistry methods. To that end, recently the group of Park reported on the combination of wet chemistry (for UCNP synthesis) and lithography (for the growth of the metal moiety);[45] this hybrid method affords nanostructures where LNPs are sandwiched between two gold plasmonic layers (**Figure 3E**). This architecture maximises the field enhancement within the LNP, and the LSPR peak could be tuned to match Yb^{3+} absorption upon controlling the diameter of the structure. These structures show above 1000-fold luminescence enhancement at low excitation power density and approximately 100-fold at high powers. Such enhancement was measured while the nanocomposite was still attached to the silicon substrate used for lithography. In fact, a smaller 50-foldluminescence enhancement was observed at high power density for the nanocomposite when dispersed in water Another interesting example is provided by the study of Fujii and co-workers, who combined wet-chemistry and thermal evaporation to prepare Y_2O_3:Yb^{3+},Er^{3+} nanoparticles with a gold cap.[74] To prepare this structure, the nanoparticles were deposited on a fuse quartz substrate, covered with a Ti adhesion layer, and finally gold deposition was accomplished at a controlled angle from the normal to the substrate. The nanostructures were then dispersed in polydimethoxysilane resin. Varying the gold deposition angle, the cap shape was tuned and, consequently, its plasmon resonance. When the LSPR approached 980 nm (Yb^{3+} absorption), the authors founda maximum green and red UC emission enhancement of 64 and 101, respectively. The authors further expanded on this topic, achieving coating of $NaYF_4$:Yb^{3+},Er^{3+} nanorods with gold caps using the same approach.[75] Also in that case, the emission

brightness was increased capitalizing on the more efficient light absorption of the nanocomposite.

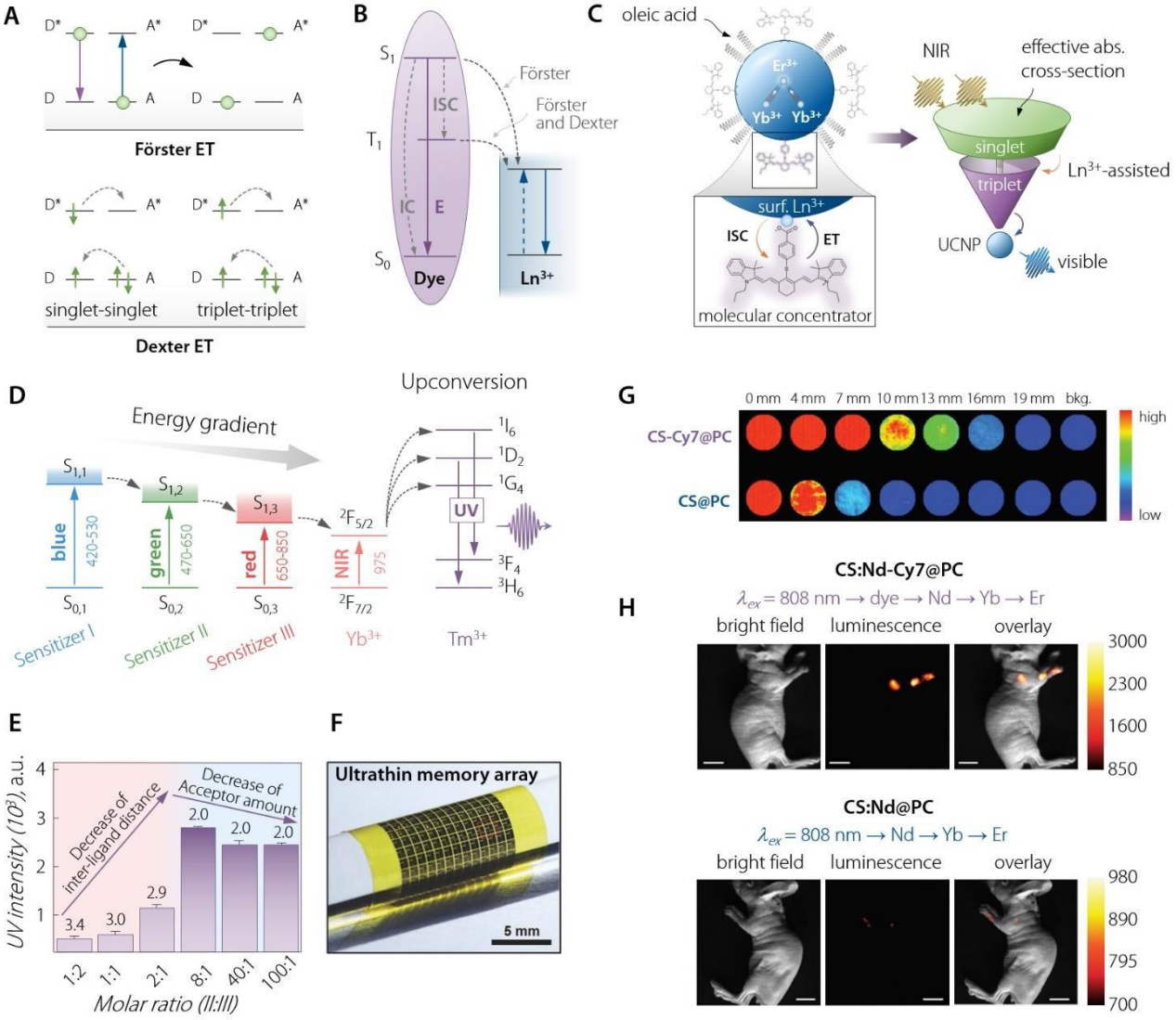

Figure 4. Organic (dye) antenna. **A)** Schematic of the energy transfer mechanisms, Förster and Dexter. **B)** Schematic illustration of nonradiative energy transfer processes from dye to Ln^{3+}. E, IC, and ISC represent the luminescence emission, internal conversion, and intersystem crossing, respectively. Adapted with permission from Ref. [76]. Copyright 2017 Royal Society of Chemistry. **C)** (**Top left**), Cartoon schematic of the dye-sensitized UCNP system, showing IR-806 bound to the UCNP surface (not to scale), and an upconversion event inside the UCNP where two excited Yb^{3+} non-radiatively and sequentially excite an Er^{3+} into a higher energy state. (**Bottom left**), magnified illustration of the interactions between IR-806 and a surface lanthanide—the heavy nucleus of the lanthanide aids in ISC from IR-806 $S_1 \rightarrow T_1$ states, allowing much more efficient T_1 sensitization of the Ln^{3+} ions within the UCNP. (**Right**), Depiction of the antenna-like nature of IR-806 in sensitizing the UCNP, conveying the much larger absorption cross-section of IR-806 relative to the UCNP, as well as $S_1 \rightarrow T_1$ISC enhancement by Ln^{3+}. Adapted with permission from Ref.[77]. Copyright 2018 Springer-Nature. **D)** Energy diagram of a three sensitizers-system and ions of the so-sensitized UCNP. The thick bars represent the energy levels, and the arrows represent the sequential energy transfer. **E)** Upconverted UV emission intensity from double-ligand UCNPs (1.6 mg mL^{-1}). Molar ratios of sensitizer II and III range from 1:2 to 100:1. The 517 nm laser power density is 25 mW mm^{-2}. The number written above the purple bars indicates the calculated

Organic antennas

Together with the use of semiconductors, this approach grantsbroadband sensitization of LNP emission, in stark contrast withthe spectrally narrow absorption lines intrinsically featured bylanthanide ions. Organic sensitization of LNPs typically involves the use of organic dye molecules anchored on the inorganic LNP surface to implement an antenna effect. Frequently the authors describe the effect of the dye as “brightness enhancement”.

Although an increased brightness is indeed the ultimate effect, the direct consequence of dye

attachment/decoration is a betterment of the absorption properties of the Ln^{3+}-doped nanoparticle. This attachment of the organic dyes to the surface of LNPs can proceed through the routes of *covalent bonding*, *electrostatic attraction*, *physical absorption,* or their combination.

Upon electromagnetic irradiation, the dye molecule is promoted to its excited singlet electronic state(s). Subsequently de-excitation takes place through several processes (**Figure 4B**):

- Non-radiative internal conversion (IC) at the dye molecule
- Intersystem crossing (ISC) between singlet and tripletstate of such molecule.
- Fluorescence emission (E).
- Energy transfer (ET) from dye molecule acting as *donor* toLn^{3+} (mostly on the surface of LNP) as *acceptor*. It involves the relaxation of dye molecules to the ground state,together with promotion of Ln^{3+} to their excited state.

Zooming into a more detailed description of the fourth step, ittypically proceeds through either Förster or Dexter non- radiative energy transfer or a combination of the two.

For a given donor-acceptor pair (**Figure 4A)** (i) Dexter mechanism is an *exchange* interaction, that involves a double electron transfer and requires a sizeable orbital overlap between the wavefunctions of organic molecule as the donor

(D) and the Ln^{3+} as the acceptor (A); (ii) Förster (or dipole– dipole) mechanism is an *electrostatic* interaction, in which thedipole moment associated with the dye molecule's state couples with the dipole moment of the 4f orbitals. In addition,dipole–multipole transfers play a non-negligible role in the sensitization of Ln^{3+} ions. [81, 82]

Both singlet and triplet states of the organic molecules may transfer energy to the lanthanide ion, possibly with the assistance of phonons. However, since the singlet state is short- lived, transfer from this latter level is often not efficient. The most likely energy transfer process to happen (ET from S_1; **Figure 4B**) leads as its outcome to the relaxation of dye molecules to the ground state S_0 and promotion of Ln^{3+} to an excited state. But it is also possible that ISC (whose likeliness isinversely proportional to the S_1–T_1 energy gap) can occur moreefficiently than the ET from S_1 just described. If that is the case,dye molecule will first switch to its triplet state (T_1), then an ETfrom T_1 to Ln^{3+} may happen. That second kind (and less likely to occur) ET can be Förster, Dexter, or both simultaneously. In themajority of the published dye-Ln^{3+} systems, emphasis is put onFörster-based description only, because of the higher ET rate from S_1 over the ISC one. Inter-distance wise, at an estimated range dye molecule–Ln^{3+} in the 1–2 nm range, Dexter ET was usually found to be negligible or, at maximum, comparable with Förster mechanism.

Albeit a selected list of representative applications and developments of the organic antenna approach for betterment of LNPs absorption is included within this section (*vide infra*), we include here as a highlight the innovative work by D.J. Garfield et al.[77] Therein, the authors managed to amplify UC nanoparticles (UCNPs) emission by enriching the molecular antenna triplets. This was accomplished by promoting ISC in the dye via adjustment of the UCNP composition. It was demonstrated that the triplet states in dye antennas critically affect the brightness and stability of dye–UCNP systems, thus providing relevant insight to overcome limitations found in previously reported materials. The IR-806-sensitized $NaYF_4$:Yb^{3+},Er^{3+} UCNPs underwent an adjustment of Gd^{3+} content, from 0 to 30%, substituting Y^{3+} ions. In particular, ISC within the dye was found to be enhanced by the larger spin– orbit coupling to Ln^{3+} ions near the surface of the UCNPs achieved by increasing the Gd^{3+} content (**Figure 4C**). Furthermore, this enriched triplet population was responsiblefor a significant amount of the energy transferred into the UCNP. The overall result was a 30-fold enhancement in UC emission. The main conclusion of this work is the possibility to concurrently optimize the LNP composition and the dye sensitization pathway to achieve maximum optical performance.

3.2.1 Rise of the concept, from the metal-organic complexes. Thebasic concept of organic molecules transferring absorbed optical energy to Ln^{3+} - no nanoparticle involved - can be tracked to the middle of last century. A seminal study by S. I. Weissmanin 1942[83] proved the efficient transfer of energy from organic ligands to Eu^{3+} ions in metal complexes. To that end, early 2000s witnessed a blooming of the field of lanthanide complexes, under the general idea of chromophores sensitizing Ln^{3+} emission (a concept also applied to supramolecular architectures and self-assembled compounds).[84] By 2007, the first report was published by J. Zhang et al. testing the conceptof an organic dye acting as antenna for lanthanide-doped (inorganic) nanoparticles.[85] This seminary paper portrayed the combination of the antenna effect provided by organic chromophores with the protection of Ln^{3+} given by an inorganic matrix. In the dawn of using antenna dyes for LNPs, the work from L. J. Charbonnière et al. must be highlighted.[86] The authors reported an increase in the emission of Eu^{3+} under 305-nm excitation of up to two orders of magnitude, as compared to the same Eu^{3+}-doped nanoparticles with no dye attached. A thorough photo-physical

study demonstrated that such large increase of the brightness of LNP's luminescence, with a corresponding long-lived excited-state lifetime, was caused bya broad absorption in the near-UV and subsequent energy transfer to Eu^{3+} from bipyCOO^- ligands tethered to the surface.

Organic antennas for UCNPs. History says that back in mid- and late 2000s, the genesis of the research interest around LNPs started with UCNPs based on the most classic Yb^{3+} (*sensitizer*)-Er^{3+} (*activator*) ion pair. The UC process is a low-output one; on top of the already described low absorption coefficient of Ln^{3+}-doped materials, the intrinsically poor efficiency of (nonlinear) UC emission is to be added. This unfortunate synergy of brightness-limiting constraints makes UC a very attractive research area to test the potential of the organic antenna approach. Obviously, the application of organic (dye) antennas in the field of UC makes it necessary to find NIR- absorbing dyes, which are able to properly funnel the NIR excitation energy to Ln^{3+} sensitizers inside the UCNP matrix.

A remarkable milestone of this bubbling trend was published in 2012, when W. Zou et al. reported an enhancement by a factorof ~3,300 of the overall sensitized UC emission of $NaYF_4$:Yb^{3+},Er^{3+} UCNPs by using antenna molecules of the NIR-absorbing IR-806 organic dye.[87] This dye was a carboxylic acid-functionalized derivative created by nucleophilic substitution of the central chlorine atom in IR-780, a commercially available cyanine dye. The use of such novel dye implied to blue-shift to806 nm of the absorption maximum of the structure (LNP + dye) from 975 nm (i.e., direct Yb^{3+} absorption) otherwise used for optical excitation of the very same LNPs with no dye attached. The extinction coefficient of IR-806 at 806 nm was measured to be ~5×10^6 times higher than that of $NaYF_4$:Yb^{3+},Er^{3+} nanoparticles at 975 nm. Interestingly, a set of photophysical control experiments demonstrated that ~50% of the photon energy initially absorbed by IR-806 is transferred to the Yb^{3+} and Er^{3+} energy-accepting ions in the $NaYF_4$:Yb^{3+},Er^{3+} core. The glaring shortcoming of the proposed system was the remarkably large energy gap between the energy levels of the dye molecule and Yb^{3+} ion. That fact limited the ET efficiency tosupport the UC process via the usual ET pathway (dye to Yb^{3+} and then to Er^{3+} emitter). Moreover, the energy mismatch between Nd^{3+}-Yb^{3+} energy levels may cause the ET performance to be undesirably temperature-dependent. Years later, G. Chen et al. introduced the concept of cascade energy UC to mitigatesuch drawback. Using ($NaYbF_4$:Tm^{3+}0.5%/$NaYF_4$:Nd^{3+} core/(active) shell UCNPs sensitized by different NIR-absorbingdyes as a model, they achieved a large enhancement in visibleUC emission, efficacious ET, and surprisingly high (~19%) quantum efficiency.[88]

As outstanding example from the materials viewpoint, in 2018the work by C. Hazra et al. pushed the limits on the spectral range of excitation wavelength for dye sensitized UCNPs.[89] In that work, the use of a water-dispersible dye absorbing above1000 nm (IR-1061) to sensitize $NaYF_4$:Yb^{3+}30%/Tm^{3+}0.5%/$NaYF_4$:Yb^{3+}10% core/active shell UCNPs was proposed for the first time. Having the goal of proofing biomedical potential, the authors managed toencapsulate the as-synthesized NIR-absorbing dye in the polyoxomer Pluronic F68 (PF-68), thus rendering the dye waterdispersible owing to the presence of hydroxyl groups. Quantitatively, a relatively modest ~3-fold enhancement in the800-nm emission of the Tm^{3+} ion was reported, from the waterdispersible IR-1061-sensitized core/active shell UCNPs via
doping of Yb^{3+} ions (10% optimal) in the UCNP shell.

to which almost half of the photons reaching Earth from the Sun belong. This active research line is very well exemplified by the work by S. Hao et al.[90] The authors built a core/shell nanoparticle, $NaYF_4$:10%Yb,2%Er/$NaYF_4$:30%Nd, sensitized with NIR-absorbing dye IR-783, and implemented it into a dye-sensitized solar cell (DSSC), achieving a 13.1% performance enhancement compared to the control cell in the absence of the UCNP converting layer. Furthermore, efficiency improvement following NIR harvesting was quantified to be >3-fold higher than the one obtained with core/shell UCNPs with no IR-783 dye attached. Importantly for technologically viable developments, upon checking the photostability, the IR-783 dye was demonstrated to be photostable under AM1.5g simulated sunlight irradiation.

In the ever-growing field of integrated photo-electronics, systems based on dye-sensitized LNPs have been also activelydeveloped. The work by J. Lee et al. is remarkable for several reasons, [78] starting from the use of a multi-dye organic antenna to sensitize (β-NaYF4:20%Yb, 0.5%Tm UCNPs. Namely, the three dyes were BODIPY-FL, Cy3.5, and IR-806), the three of them having in common their composition made of an energy harvesting aromatic fluorophore and a carboxylic acid for linkage to the UCNP. This game-changer approach widens the photon absorption window of such nanoparticles, from solely the NIR range (975 nm, when relying on just Yb^{3+} as sensitizer)to the entire visible and NIR-I range (450–975 nm) (**Figure 4D**).Such expansion of the excitation range, encompassing photons that cannot be used in conventional UCNPs, maximized the utility of such Yb^{3+}/Tm^{3+}-doped UCNPs**.** That is because a large photo-absorption bandwidth with high absorption coefficients increases the upconverted output emission intensity in the UVrange. Moreover, the authors walked the extra mile in terms of material engineering, optimizing the sensitizer-ligand distanceand the ratio between the different organic dyes, thus furtherincreasing the efficiency of the sequential ET and UC processes(**Figure 4E**). Finally, the third exciting aspect of the work lies inthe application of such fine-tuned nanosystem, in liaison with ultraviolet (UV)-responsive photo-acid-generators (PAGs), as anew information security module in data storage devices with a function of unrecoverable data erasure. Because of the ultrathin nature of the so-built electronics, the entire system is deformable and can be integrated on various curvilinear surfaces including the human skin (**Figure 4F**).

Not all the outstanding examples of organic antennas improving absorption for LNPs that we can lately found are developed inUC systems. The current growing trend of developing NIRemitters for biomedical imaging - owing to the deeper penetration, better optical contrast, and low tissue autofluorescence characterizing such “transparency window” -finds in LNPs a fertile ground. NaYbF /NaYF :Nd^{3+}60%

cent representative developments on organicantennas sensitization of LNPs

There are diverse fields of application of the organic antenna approach for LNPs absorption betterment. In photovoltaics, the UCNPs have been much sought after to expand the spectral working range of solar cells towards the NIR, the spectral range

nanoparticles were coupled with high-PLQY Cy7 dye in the work by Q. Liu et al. in 2018.[79] By the imaginative approach of buildinga pure $NaYbF_4$ emitter core, authors augmented the Nd^{3+} doping concentration up to 60% - appreciably higher than in the case of most reported dye-sensitized systems - in the outer shell. That architecture favoured the optically absorbed energy being transferred from the sensitizer (Cy7) to emitters (Yb^{3+}) via intermediate ions (Nd^{3+}) - the overall benefit being offered by a significant increase in the absorbance of the LNPs. Therefore, brightness was increased translating into a deeper imaging penetration (**Figure 4G**). The relevance of this report lies also inhow the water-solubility and biocompatibility of the nanosystem were addressed by wrapping the Cy7 dye- core/shell composite in phosphatidylcholine. That way, two ofthe key points of concern for biomedically oriented LNPs weretaken care of. This NIR emitting (centred on 980 nm) material was applied *in vivo*, proving itself a promising imaging agent for fluorescence-guided surgery, by way of its application to assist in the procedure of peritumoral lymph node dissection. Notwithstanding the achievements of this paper, in light with the critical approach of this review, it is also worth noting thatthe characterization experiments performed by the authors shown that coating with an inert shell would make energy transfer efficiency from Cy7 to Nd^{3+} relatively weak. This happens because the undoped outer shell increases the physical distance between (*donor*) organic molecules and (*acceptor*) Ln^{3+} ions, thus hindering ET between the two species. Such incompatibility makes impossible to simultaneously implement organic antennas (for absorption betterment) together with the growth of an undoped outer protective shell(nowadays, a widely used approach to improve the LNPs quantum yield when in colloidal suspension). That constitutes a limiting issue within the framework of LNP´s achievable brightness by organic antennas approach, a matter discussed further in this review (*vide infra*).

If directing attention to best NIR-absorbing organic dyes, the above mentioned Cy7 has indeed made possible in vivo imaging even for UCNPs acting as imaging probes by emitting in the visible. That constitutes a remarkable feature, when considering the lower tissue penetration depth of that shorter wavelengthrange. Nd^{3+}-based UCNPs sensitized with Cy7 demonstrated, as shown in the report by X. Zou et al, in vivo lymphatic imaging at 540 nm under excitation at 808 nm (**Figure 4H**).[80]

Finally, the report from W. Shao et al. in 2016 should also be analysed within the current research trend looking to developdownshifting LNPs which emit at longer wavelengths (NIR-II, meaning 1000−1700 nm spectral range).[91] The authors achieved NIR-II increased emission, aiming for much deeper *in vivo*penetration depth (because of the lower tissue extinction at those wavelengths), better optical contrast and high signal-to-noise ratio (owing to the low tissue autofluorescence). The $NaYF_4$:Yb^{3+}/X^{3+}/$NaYbF_4$/NaYF4:Nd^{3+}, X = null, Er, Ho, Tm, or Pr)$_{core/shell/shell}$ system, with indocyanine green (ICG) attachedto the surface, was designed to create a cascade ET pathway upon 700−860 nm optical excitation: ICG→Nd^{3+} (outer shell)→Yb^{3+} (inner shell) →Yb^{3+}/X^{3+} (core). The ICG antenna not only enhanced the overall brightness of the multiple-line emission of the LNPs by ∼4 time, but also provided a much broader excitation band than the LNPs had just by themselves.The proof of concept of NIR-II bioimaging was extended *in vivo*, by means of subcutaneous injection of an aqueous suspension

of phospholipid-encapsulated ICG-sensitized core/shell/shell LNPs which allowed imaging in a mouse.

3.2. Semiconductors as light harvesters

The use of SCNs for the sensitization of Ln^{3+} emission follows the same principle of organic antennas: the semiconductor moietyshould be able to absorb the optical energy and transfer it to the Ln^{3+} ions. The pivotal difference from the case of organic antennas is that the role of the dye's triplet state is herein played by the semiconductor's excited states. These can be localized excitonic levels, inter-bandgap levels, and charge trapstates **(Figure 5A**). SNCs have a molar absorption coefficient generally slightly larger than dyes (up to 10^6 vs up to 10^5 $M^{-1}cm^{-1}$).[92] However, the smaller size of dye molecules could mitigatethis partial shortcoming, since it is plausible to think that moredye molecules rather than SNCs can be accommodated on thesurface of a LNP (if decoration of a LNP with SNCs is the pursued approach). On the other hand, in the case of using SNCs, the final material is fully inorganic and hence it is less prone to photobleaching and degradation in harsher environments. Aside from these points above, a fair comparison should also include the efficiency of the transfer between the light harvesting moiety (dye or SNC) and the lanthanide ion. Unfortunately, the very limited availability of these numbers makes it difficult to fairly compare the performance of the twoapproaches from this point of view.
Sensitization of Ln^{3+} through SNCs was accomplished via different approaches, such as coupling of SNCs and LNPs, doping of Ln^{3+} in a SNC, and synthesis of core/shell SNC/LNP structures. Albeit these methods rely on a similar operation principle (**Figure 5A**), they require attention to different variables.

Coupling of LNPs and SNCs. The main advantage of this method compared to doping Ln^{3+} in SNCs is the possibility to separately control the properties of the two nanoparticles. Moreover, the surface chemistry of the two species can be tuned independently depending on the coupling strategy one wants to pursue. Two particularly relevant examples are represented by the amalgamation of NIR-absorbing SNCs of Ag_2S[93] or Ag_2Se[94] with LNPs to achieve brighter NIR-II or visibleUC emission, respectively. Zhang et al. synthesized the final hybrid Ag_2S-$NaYF_4$:Yb^{3+},Er^{3+} nanostructure leveraging the electrostatic interaction between the positively charged surface of ligand-free LNPs and the carboxylic group of mercaptopropionic acid (MPA) on the surface of Ag_2S SNCs. The resulting LNPs decorated with SNCs displayed a 17-fold increase of Er^{3+} emission intensity (at 1550 nm) under 808-nm irradiation compared to direct 980-nm excitation of Yb^{3+} (**Figure 5B**). The authors also achieved in vivo tumour imaging in NIR-II under 808 nm excitation. They modified the surface of LNPs with a glutathione-cleavable peptide; after cleavage took place in the tumour microenvironment, maleimide-modified Ag_2S SNCs injected in the mouse could bind to the LNPs via a "click" reaction, thus enabling the semiconductor mediated sensitization of Er^{3+} emission. The result is an elegant demonstration of in vivo tumour imaging using a two-stage injection strategy which allows increasing the emission intensity of the LNP on demand. *En route* to the development of this combined imaging probe, the authors also explored the effectof growing a protective shell on the LNP. The observed trend

echoes the results observed with dye sensitization, with the luminescence enhancement through SNC decreasing almost linearly with the thickness of the shell. This is the result of the

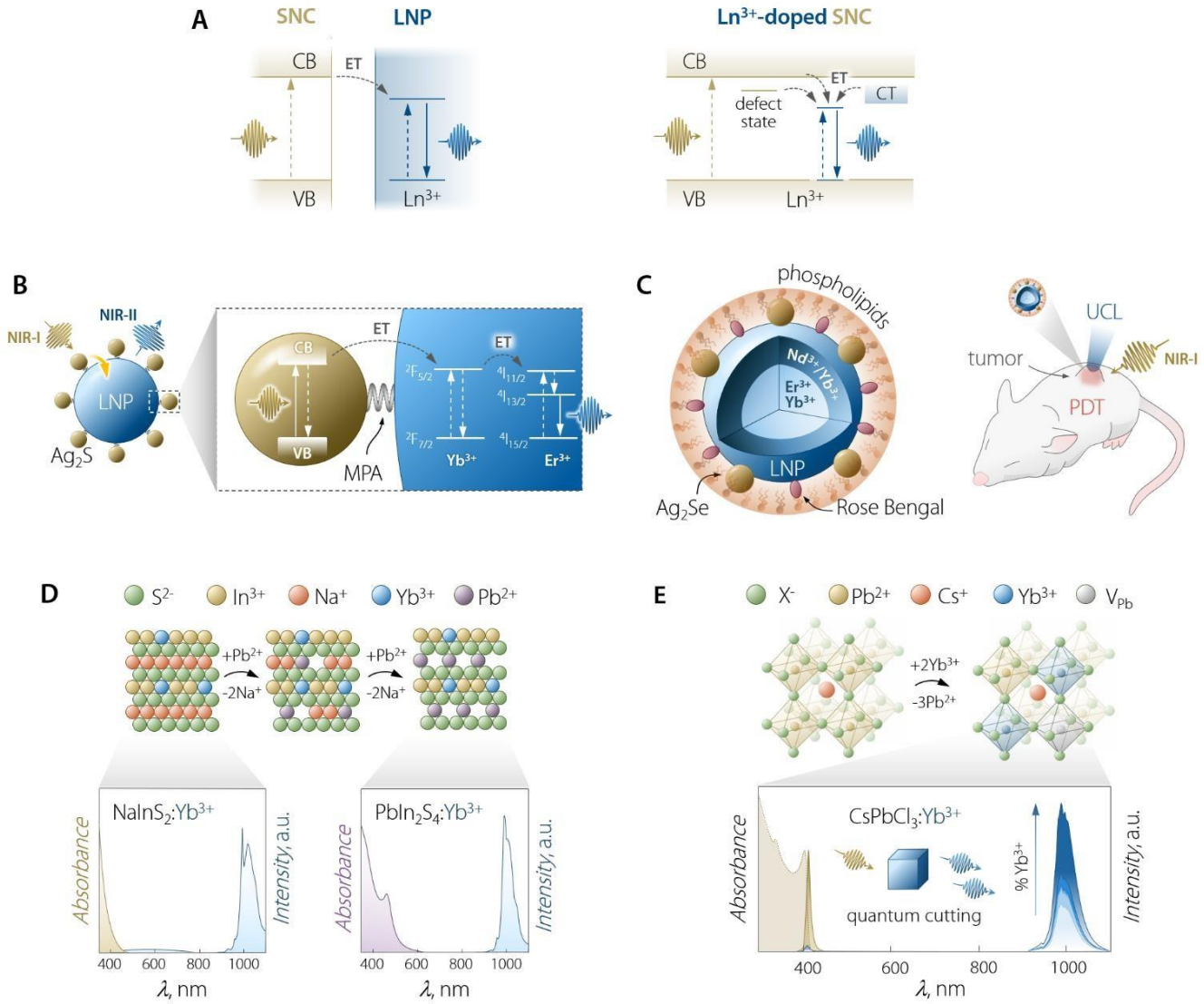

igure 5. Use of SNCs to increase the brightness of lanthanide emission. **A)** Partial energy level diagrams to illustrate the sensitization mechanism between conjugated SNC and LNP moieties (left) and in the case of Ln^{3+}-doped SNC (right). In the latter case, CT stays for charge transfer state; dark yellow arrows indicate the ET processes and vertical lines are electronic transitions. **B)** Scheme of Ag_2S SNC-decorated Yb^{3+},Er^{3+}-doped LNP along with the proposed energy transfer mechanism responsible for the sensitization of lanthanide NIR emission. MPA = 3-mercaptopropionic acid. Adapted with permission from Ref.[93]. Copyright 2020 American Chemical Society. **C)** Scheme and means of operation as an optical probe and PDT agent of the Ag_2Se-LNP-Rose Bengal composite encapsulated in phospholipids. Adapted with permission from Ref.[94]. Copyright 2019 American Chemical Society. **D)** Preparation of Yb^{3+}-doped $PbIn_2S_4$ SNCs and their optical properties. The cation exchange process to transform $NaInS_2$ into $PbIn_2S_4$ entails the substitution of two Pb^{2+} ions for each Na^+. Both $NaInS_2$:Yb^{3+} and $PbIn_2S_4$:Yb^{3+} feature host sensitized Yb^{3+} emission around 1000 nm, however, upon passing from $NaInS_2$ to $PbIn_2S_4$, the absorption extends to longer wavelength, covering a good part of the visible spectrum. Adapted with permission from Ref.[95]. Copyright 2017 American Chemical Society. **E)** Lanthanide doping scheme in Pb^{2+}- based halide perovskite SNCs along with the absorption and emission spectra of CsPbCl3:Yb^{3+} SNCs doped with increasing amounts of lanthanide ion (from 0 to 7.4%). Adapted with permission from Ref.[96]. Copyright 2018 American Chemical Society.

increased distance between the doped Yb^{3+} ions in the core (acceptors) and the Ag_2S SNCs tethered to the outer surface (donors). This assumption was confirmed by the regain inluminescence enhancement upon doping Yb^{3+} ions also in the overgrown outer shell, thus enabling efficient SNC-to-Yb^{3+} ET again. It is interesting to note that the overall PLQY of the bestperforming sample only amounts to 0.16%. On the bright side,the composite retained up to 70% of the emission intensity upon continuous 808-nm irradiation for 60 min, in stark

opposition to the 98% drop experienced by the analogue system featuring IR-806 dye molecules in place of Ag_2S SNCs. In a similar fashion, Song et al. prepared hydrophilic $NaYF_4$:Yb^{3+},Gd^{3+},Er^{3+}/$NaYF_4$:Yb^{3+},Nd^{3+} core/shell LNPs and co- encapsulated them with hydrophilic Ag_2Se SNCs in micelles of phosphatidyl choline (**Figure 5C**). Upon optimizing the SNC content in the micelles, the authors observed an 18-fold increase of the UC emission. Aside from using the system for imaging purposes, the authors displayed its suitability as a photodynamic therapy (PDT) agent when Rose Bengal (RB) was co-encapsulated in the micelles. In fact, the construct showed reactive oxygen species generation upon 808 nm irradiation, thanks to the UC-mediated excitation of RB. It is also likely that the system displays NIR-II emission due to the presence of Er^{3+}, which could be harnessed for imaging purposes – as in the case of previously discussed Ag_2S-$NaYF_4$:Yb^{3+},Er^{3+}. However, the authors did not explore this possibility. It is important to point out that the authors also investigated the photostability of the Ag_2Se SNCs versus a solution of IR-806 (a dye presented in the previous section as a suitable organic antenna) under 808 nm excitation. They observed a 10% emission intensity decrease in the case of SNCs, while the dye almost completely photobleached. This evidence corroborates the higher robustness of LNP-SNCs systems versus those based on organic antennas for Ln^{3+} sensitization.

Nonetheless, as mentioned above, one of the main disadvantages of this approach lies in the necessity of the SNCs to be in close proximity to the sensitizer ions for the ET to effectively take place. This means that only superficial ions in the LNP can accept energy from the SNCs. This reduces the possibility of growing a passivating shell on the LNP, as mentioned also earlier in this review in the case of dye- sensitization of LNP emission (see Section 3.2.3). All these considerations have been demonstrated also in the reverse case of LNP-to-SNC ET,[97, 98] and they pose limitations in the design of the final nanostructure.

3.2.1. Doping of Ln^{3+} in SNCs. This approach yields a single entity rather than a composite nanostructure where two or more particles are bound together. However, this compactness comes with the cost of more stringent requirements to meet in the material design and from a synthetic standpoint. We have discussed in detail this specific approach in a recent dedicated Review,[99] therefore here we will only outline the main aspects to be considered. Notably, the following considerations are valid generally when attempting the doping of any nanoparticle with Ln^{3+} ions. First, a host material apt for substitutional Ln^{3+} doping should feature cationic sites with high coordination number (CN),[100] such as those with octahedral or cubic geometries. In addition, similar ionic radius and oxidation state favour the substitution of the native cation in the SNC with Ln^{3+}. Once the suitable host material has been chosen, the preparation of Ln^{3+}-doped SNCs could proceed through several synthesis methods, such as growth doping,[101] nucleation doping,[102] cation exchange,[103] and diffusion doping[104]. All these methods have in common the need to control the reactivity of the different ions in the reaction environment so to promote the incorporation of Ln^{3+} in the lattice. This is no easy task and often a combination of coordinating molecules should be employed to ensure that Ln^{3+} ions successfully enter and resides in the SNC lattice. Clearly, all these considerations should be complemented by attention to the relative energetic position of the semiconductor excited states and the Ln^{3+} emitting state, as previously mentioned. This set of requirements makes the preparation of Ln^{3+}-doped SNCs challenging. Moreover, there is an element of serendipity that is constituted by the possible

defects introduced by the doping of Ln^{3+} in the lattice. These defects can behave as localized trap, introducing interband gap trap states for charge carriers that either contribute to non- radiative recombination or act as effective bridge between host and doped Ln^{3+}.

Early attempts to prepare Ln^{3+}-doped SNCs focused on the useof binary semiconductors, such as CdS,[105] CdSe,[106, 107] andZnS[108]. However, those lattices are far from ideal in this context, since therein Cd^{2+} and Zn^{2+} occupy low-CN site (tetrahedral). Moreover, those ions feature different size and oxidation statecompared to Ln^{3+}. In fact, most of the works attempting Ln^{3+} incorporation in the SNC lattice mainly report evidence of surface absorption of the dopant ions.[109] Some success was obtained by the group of Meijerink, who managed toimmobilize Yb^{3+} ions on the surface of CdSe SNCs via ionadsorption followed by the overgrowth of a thin Se layer.[107] Numerous are the studies on the incorporation of Ln^{3+} in oxide- based semiconductor nanoparticles, such as ZnO,[110] TiO_2,[111] In_2O_3,[112] and Ga_2O_3.[113] Although host sensitization is achieved in those hosts, the efficiency is generally poor, and the absorption of the semiconductor moiety lies in the UV-Vis part of the spectrum. Interestingly, Gamelin and co-workers reported the incorporation of Ln^{3+} in the lattice of colloidal ternary SNCs (**Figure 5D**).[95] Their approach involved the use of $NaInS_2$ as host material: a ternary semiconductor where In^{3+} resides in an octahedral environment. The similar ionic radius of this cationcompared to Ln^{3+}, along with same oxidation state (3+), allowed for effective incorporation of Yb^{3+} in the lattice. The advantageof using a ternary system where cations with different properties (i.e., Na^+ and In^{3+}) granted the possibility to performselective cation exchange to fine tune the optical properties ofthe Ln^{3+}-doped SNCs. The authors showed that Na^+ can be substituted by Cd^{2+}, Ag^+, and Pb^{2+}. Exchange with the latter cation afforded $PbIn_2S_4$:Yb^{3+} SNCs, which exhibited extended visible absorption and a maximum PLQY of 5%.

Other host materials that grant effective Ln^{3+} doping are alkaline-earth semiconductors (AESs) like CaS and SrS. [114, 101, 115, 116] The large cationic radius of the alkaline earths, along with their high CN allows for their substitution by lanthanides. Often Ce^{3+} is doped in these hosts, while europium takes its divalentstate. Both Ce^{3+} and Eu^{2+} feature allowed 4f-5d electronic transitions, and hence relatively good light absorption – an exception to the cases discussed thus far.[117] Hence, albeit hostsensitization is observed, generally efficient direct excitation ofdoped lanthanide ions is realized. For instance, Zhang et al. recently prepared CaS:Ce^{3+},Er^{3+} and CaS:Ce^{3+},Nd^{3+} featuring NIR emission under UV-blue excitation. Energy transfer from Ce^{3+} to the second Ln^{3+} enabled bright emission (9.3 and 7.7% respectively for Er^{3+} and Nd^{3+}). After transferring these LNPs towater with the aid of phospholipids, the authors managed to sense H_2O_2 and H_2O_2-producing disease marker xanthine in water. Detection of those species was afforded by quenching of the Ln^{3+} emission in the presence of hydrogen peroxide.

This section would not be complete without mentioning halideperovskites. In the past few years, semiconductors of the family $CsPbX_3$ (where X = Cl, Br, I) have become the staple for Ln^{3+} doping in SNCs, with unmatched results in terms of host sensitized photoluminescence efficiency.[100] Halide perovskitesin general feature octahedral sites that offer the ideal coordination environment for Ln^{3+}. In lead-based systems, doping with Ln^{3+} proceeds through the substitution of three Pb^{2+} for every two incorporated lanthanides.[96, 118] To maintain a charge balance, a Pb^{2+} vacancy (V_{Pb}) is also introduced. The mostenergetically favourable configuration of the resulting defect complex (Ln^{3+}-V_{Pb}-Ln^{3+}) is shown in (**Figure 5E**). Hence, Ln^{3+} doping of halide perovskites proceeds through the creation ofdefects and the possibility to successfully dope this material hinge on the tolerance that it possesses towards defects, both structure- and emission-wise.[119, 120] Several Ln^{3+} (Ce^{3+}, Sm^{3+}, Eu^{3+}, Tb^{3+}, Dy^{3+}, Dy^{3+}, Er^{3+}, Yb^{3+}) were doped in $CsPbCl_3$ SNCs byPan et al.,[121] observing increased overall PLQY (exciton + Ln^{3+} emission) compared to the undoped system. Stunningly, the PLQY in the case of Yb^{3+} doping overcame 100%. Because of their high conversion efficiency and the ideal overlap of Yb^{3+} emission with silicon absorption, Yb^{3+}-doped halide perovskites are thus envisioned as ideal conversion materials in photovoltaic devices. Indeed, conversion layers for silicon and $Cu(In,Ga)(S,Se)_2$ cells[122, 123] and quantum cutting luminescent solar concentrators (QC-LSC) have been prepared using Ln^{3+}- doped lead halide perovskite SNCs. This quantum cutting phenomenon was further investigated by Milstein et al., who described the quantum cutting mechanism with the help of low temperature photoluminescence study on La^{3+}-doped SNCs.[96] The authors explained the quantum cutting as assisted by shallow defect states below the conduction band, effectively bridging the electronic states of the SNC and the Ln^{3+}. In a following study, Li et al. modelled this quantum cutting phenomenon and explained it in light of a higher density of states at the CB edge featured by the Pb^{2+} sitting close to the Yb^{3+} ions; this favours strong localized absorption and prompttransfer of the energy to the two nearby Yb^{3+}.[118] Ln^{3+}-doped lead-based perovskite SNCs were also used for preparing with-light emitting diodes, wherein blue-emitting GaN chips where coated with polymeric dispersions of, e.g., $CsPbCl_3$:Ce^{3+},Eu^{3+}[121] or

$CsPbCl_{1.8}Br_{1.2}:Ce^{3+},Mn^{2+}$.[124] Despite of Pb^{2+}-based halide perovskites' showcasing excellent luminescent performance, the presence of lead in their composition, in hand with the poor chemical resistance towards moisture, poses major concerns in terms of toxicity and environmental impact.[125] Ln^{3+}-doping has been shown to improve the stability of $CsPbX_3$,[126] but their foreseeable applicability remains limited mainly to water-free environments. Doping of Ln^{3+} in other lead-free mixed perovskites has been performed too, using hosts like halide double perovskites (e.g., $Cs_2AgInCl_6$[127] and $Cs_2AgBiCl$ [128]) and $Cs_3Bi_2Br_3$.[129, 130] To that end, Eu^{3+}-doped SNCs of the latter material have been prepared by Ding et al., who employed them in aqueous media for Cu^{2+} detection: a rare instance of use of perovskites in water.[129] However, the emission efficiency of these systems is lower compared to the one featured by Pb^{2+}- containing ones. Lastly, the absorption of halide perovskites generally cannot be effectively tuned towards the red-NIR part of the spectrum, thus further limiting the versatility in terms of working wavelength range.

Despite the challenges of doping Ln^{3+} in SNCs an additional advantage of this avenue is the possibility to exploit host-to- metal charge transfer (CT) phenomena to sensitize the activator luminescence.[131, 132] According to the model proposed by Dorenbos[133] (and validated several times experimentally), Ln^{3+}ions that are more likely to give rise to CT are Eu^{3+} and Yb^{3+}, followed by Sm^{3+} and Tm^{3+}. This is because of the lower-lying ground state of their divalent form (Ln^{2+}) compared to other lanthanides. This subject is rather complex, and its thorough explanation lies beyond the scope of the present Review. The interested reader is redirected to the body of work from Dorenbos (see for example Ref. [134]). The important aspect to consider is that when Ln^{3+} are doped in hosts composed of relatively polarizable anions (such as S^{2-} and Se^{2-} as opposed toO^{2-} and F^{-}), the absorption corresponding to the CT band occurs at lower energies. This observation opens the door to the possibility of tuning the position of CT-related light absorptionby controlling the host composition.

Lastly, this approach for combining Ln^{3+} and SNCs allows for core shell architectures to be prepared. Passivation of the surface becomes therefore possible, aiming for higher PLQY. We foresee exciting scenarios ahead pursing this avenue.

3.2.2. Core/shell architectures. A unique case is represented by the work of Swabeck et al., where a YF_3:Yb^{3+} shell was grown over an InP SNC core.[135] Passivation of the system with a further shell of LuF_3 alleviated solvent molecule-induced quenching. This approach allowed achieving Yb^{3+} emission under 440 nm excitation thanks to ET from the SNC core to the Yb^{3+} ions in the YF_3 shell with PLQY between 0.1-0.5%. The sensitization appears to proceed via the involvement of an intermediate trap state (likely an Yb^{3+}-induced surface state), which acts as a bridge between InP excited states and the lanthanide ion. This claim was supported by the observation of Yb^{3+} emission also under excitation with 760 nm light, a wavelength corresponding to the energy of the trap-related emission recorded upon 440 nm excitation.
We foresee that possibly structures with the reverse architecture could be prepared in the future, where LNP represents the core and a shell of semiconductor material is overgrown. The shell would act not only as a sensitizer moiety,but simultaneously as a protective barrier for the emitting Ln^{3+}ions against quenchers (i.e., molecules with high-energy vibrations). Further shelling could be performed on the first semiconductor shell, thus additionally reducing non-radiative losses.

4. Conclusion and perspective

In this Review, we have assessed the state of the art of three families of approaches to improve the brightness (mainly by increasing the absorption capability) of lanthanide-doped nanoparticles, namely the use of *i)* plasmonic species, *ii)* organic antennas, and *iii)* semiconductor nanocrystals. From our critical literature survey, we can draw several general conclusions:

- The interest around the production of brightly emitting nanoparticles based on lanthanide ions is vivid. Efforts towards this direction are driven by the possibility of broadening the applicability of these unique luminescent species in fields such as lighting, photovoltaics, and bioimaging.
- Betterment of the light absorption properties of lanthanideions appears to be the decisive step to undertake in pursuitof increased emission brightness of these species. Strategies to achieve this goal are constantly being honed both from aphysical and chemical standpoint. Better understanding ofthe mechanisms involved in brightness enhancement by way of absorption betterment allows for a more rational andeffective design of the material. On the other hand, new materials and synthesis strategies are being proposed, thus opening fan of new opportunities.
- Despite the advancements witnessed in the preparation of more intensely emitting lanthanide-based nanoparticles, we are far from the performance and reliability of other luminescent species, such as fluorescent small molecules, quantum dots, or even lanthanide complexes. This leaves plenty of room for improvement in terms of brightness enhancement as well as chemical and photostability.

Regarding the specific strategies discussed in this Review, the following conclusions have been reached

- Coupling with plasmonic materials is one of the most exploited approaches to enhance the emission intensity oflanthanide-based nanoparticles. Yet, in colloidal systems the degree of control that can be exerted on the reciprocal position of the two moieties is limited. Combination of wet-chemistry methods and metal deposition has already proven a useful hybrid approach to prepare unique architectures. In those nanosystems the

electromagnetic field is concentrated within the lanthanide-doped nanoparticle, thus allowing for maximum luminescenceenhancement. It is expected that similar results can be achieved harnessing methods to decorate selectively different sites of plasmonic nanostructures.[136] Lanthanide-doped material can be deposited, for instance, at the tip ofgold nanorods, where the longitudinal plasmonic mode results in maximal localized enhancement of the electromagnetic field. On top of that, the use of plasmonicmaterials other than noble metals should be further investigated. For example, materials with plasmonic resonance located deeper in the NIR (e.g., >1400 nm) couldbe used to enhance the absorption and/or emission of lanthanide ions at those wavelengths, which are relativelyunexplored. Copper chalcogenides, indium tin oxide, and LaB_6 nanoparticles could serve that purpose. We also observed a lack of studies where the lanthanide-doped moiety is optimized in terms of dopant type, concentration, and relative positioning. The mastery achieved in preparing complex structures with multiple shells, wherein different dopants are spatially segregated for maximum optical performance, has grown in the past few years.[137, 138] Therefore, it should be employed also in the design of nanomaterials with even brighter plasmon-enhanced luminescence. We also note that the body of literature

dealing with brightness enhancement of LNPs by betterment of the absorption capabilities of Ln^{3+} is limited. This is unfortunate since this approach is the one anticipated to yield higher enhancements, and thus more efforts should be put in this direction. One of the possible battlefields where nanostructures based on LNPs and PNPs could be deployed is biomedicine, for theranostic (therapeutic +diagnostic) purposes. Enhanced upconversion luminescence and downshifting emission can respectively be harnessed to photoinitiate chemical reactions *in situ* and imaging, respectively. However, the presence of the plasmonic part could be a double-edged sword, owing to its light-to-heat conversion capability: if, on one hand, this effect can be harnessed for photothermal therapy, on the other side unwanted and uncontrolled heating can be generated upon irradiation.

- The most pressing shortcomings toward the consolidation of the use of organic antennas for addressing the low absorption from LNPs are basically three. Firstly, opting for this approach (absorption enhancement) limits the possibility to prepare nanoparticle' architectures with an undoped shell outer shell (improvement of quantum yield through quenching suppression). The separation imposed by the undoped shell between the Ln^{3+} and the solvent nanoparticle's surface aims to keep away quenching sources (due both to surface defects and solvent molecules with vibrational modes resonant with Ln^{3+} transitions). But such distance of Ln^{3+} from the surface where organic molecules anchor makes the antenna approach non-viable, as ET requires the involved species to be at close range. A possible solution to this conundrum could surge from the use of an optically active organic polymer able to act as antenna for Ln^{3+} and simultaneously providing a strong isolation to those very same Ln^{3+} from vibrational modes of solvent (water) molecules.

  The second limitation is directly related to the structural stability and long-term robustness preserving the integrity of the whole antenna-nanoparticle construct. In the majority of published reports, the binding stability of the dye onto the nanoparticle surface remains largely a matter of pending further study, along with the unknown photostability of the dye-sensitized LNP. To that end, no comparative studies have been systematically performed for the most functional "anchoring" methods (i.e. covalent bonding, electrostatic attraction, and physical absorption). In particular, the unknown stability of the bond between the dye and the nanoparticle curbs the application of these nanocomposites in the *in vivo* biomedical arena: indeed, upon injection in the specimen, those LNPs would find themselves in a potentially aggressive environment that could possibly induce detachment of the dye molecules.

  Lastly, the third relevant factor imposing constraints is the number of dyes per nanoparticle. In published works, tis number has often been reported to be less than 1000:1, thus posing a threshold the light harvesting ability of dye- sensitized LNPs. In other words, it seems to exist an upper limit of dye molecules per nanoparticle above which the molecules are more likely to transfer energy between them than to the Ln^{3+} inside the LNP matrix.

  As a general comment, there is still a sort of "thematic scope gulf" keeping disciplines away between materials scientists/physicists studying lanthanides and chemists working on colloidal dispersions. However, it is reasonable to think that this gap will continue being gradually bridged, especially when considering previous relevant cases such as the very travelled research road of dye-sensitized semiconductor solar cells.

- The research line on the use of semiconductor materials to sensitize the emission of lanthanide ions is by far the one that is gaining greater momentum, thanks to the advent on the scene of halide perovskites. The optical and structural properties of these materials make them utterly suitable for the preparation of Ln^{3+}-doped nanoparticles with bright emission. Provided, that lead-based species are the one performing the best, future effort should be put in the development of LNPs based on heavy metal-free materials and resistant to moisture (hence more broadly applicable in aqueous environments). Bismuth-based and halide double perovskites are amongst the most promising materials in these regards. Following this path, on one hand concerns about the toxicity of the material would be mitigated. On the other, more stable and water-resistant species will ensure their broader applicability in field such as light- emitting diodes, photovoltaics, and biomedicine. Aside from perovskites, it is foreseeable that novel, efficient lanthanide-doped semiconductor nanocrystals could be produced leveraging the strategy of ion exchange – following the example set by the group of Gamelin.[95] Ternary semiconductors represent the ideal canvas for this approach, as they allow orthogonal manipulation of their composition (i.e., selective exchange of one or the other metal ion). Once these strategies will be mastered, taking one page from the book of quantum dots, preparation of core/shell architectures is the natural successive step. The minimization of surface quenching phenomena that will result is envisaged to increase the emission brightness of doped lanthanides to an even higher degree. Core/shell structures where the core is a LNP and the shell is constituted of semiconductor material are also expected to be designed (although the lattice mismatch between the materials involved might pose serious limitations to the realizability of these structures). Regarding other

strategies, coupling of pre-synthesized semiconductor nanocrystals and lanthanide-doped nanoparticles could provide a meansto tune more finely the optical properties of the two moieties in a separate way. On the negative side, the nature of the interparticle energy transfer mechanisms involved inthe sensitization process poses limits in terms of maximum distance between the energy donor (semiconductor nanocrystal) and the acceptors (lanthanide ions doped in the nanoparticle). Notwithstanding this, it is often easier toprepare such composite structures rather than pursuing lanthanide doping in semiconductors, given the knowledgegained over the recent years of nanoparticle surface

functionalization. This knowledge also allows to agilely tune the affinity (i.e., dispersibility) of the composite towards different environments depending on application sought after; a task more challenging in the case of using organic dyes – most of which are not hydrophilic. Consequently, weproffer that coupling of semiconductor nanocrystals and lanthanide-doped nanoparticles could bring exciting resultsin the next few years, particularly in the biomedical context.

All in all, the journey in chase of brighter lanthanide-doped nanoparticles exhibit several opportunities and it is far from being at its end. While the avenues described above have beenwalked so far independently, it is also possible that they will intersect, joining forces quite literally *for a brighter tomorrow*.Case in point, coupling of plasmonic nanoparticles and lanthanide-doped nanocrystals can be performed with the goal of simultaneously profiting from the host sensitization and Purcell effect. Decoration of lanthanide-doped nanoparticles with both plasmonic species and organic dyes could be performed too. These are just some examples, but the list of combined methods (currently available and newly developed ones) is expected to become quickly longer.
As we have mentioned throughout Section 3, the application fields that would mainly benefit from availability of lanthanide- doped inorganic nanoparticles are photovoltaics, lighting, sensing, and biomedicine. Of course, each area requires specific requirements to be met in terms of optical and physicochemical features, as well as toxicity profile of the nanosystem. For thisreason, it is plausible to think that different strategies will provide species suitable for different applications. What we are convinced of is that lanthanide-doped nanoparticles madebrighter via the methods herein reviewed will play a pivotal role in several fields.

Conflicts of interest

There are no conflicts to declare.

Acknowledgements

Authors thank Prof. A. Fernández-Domínguez (UAM) for helpful discussion about plasmonic-related concepts. R. M. is gratefulto the European Commission for the European Union's Horizon2020 research and innovation program, Marie Skłodowska- Curie Grant agreement No. 797945 "LANTERNS". A. B.acknowledges funding from Comunidad Autónoma de Madridthrough TALENTO grant ref. 2019-T1/IND-14014. This work was partially supported by the Ministerio de Economía y Competitividad de España (MAT2016-75362-C3-1-R), by the Ministerio de Innovación y Ciencia (PID2019-106211RB-I00) bythe Instituto de Salud Carlos III (PI16/00812), by the Comunidad Autónoma de Madrid (B2017/BMD-3867RENIMCM), and co- financed by the European Structural and Investment Fund. Additional funding was provided by the European CommissionHorizon 2020 project NanoTBTech.

References

1. M. Poliakoff, A. D. J. Makin, S. L. Y. Tang and E. Poliakoff, *Nat.Chem.*, 2019, **11**, 391-393.
2. R. Marin, G. Brunet and M. Murugesu, *Angew Chem Int Ed Engl*, 2019, DOI: 10.1002/anie.201910299.
3. D. N. Woodruff, R. E. Winpenny and R. A. Layfield, *Chem. Rev.*, 2013, **113**, 5110-5148.
4. S. F. Himmelstoss and T. Hirsch, *Methods Appl. Fluoresc.*, 2019, **7**, 022002.
5. C. D. S. Brites, S. Balabhadra and L. D. Carlos, *Adv. Opt. Mater.*, 2018, **7**, 1801239.
6. B. del Rosal, E. Ximendes, U. Rocha and D. Jaque, *Adv. Opt. Mater.*, 2017, **5**, 1600508.
7. A. Skripka, V. Karabanovas, G. Jarockyte, R. Marin, V. Tam, M.Cerruti, R. Rotomskis and F. Vetrone, *Adv. Funct. Mater.*, 2019, **29**, 1807105.
8. Z. Chen, X. Wang, S. Li, S. Liu, H. Miao and S. Wu, *ChemPhotoChem*, 2019, **3**, 1077-1083.
9. F. Vetrone, R. Naccache, A. Zamarron, A. Juarranz de la Fuente, F. Sanz-Rodriguez, L. Martinez Maestro, E. Martin Rodriguez, D. Jaque, J. Garcia Sole and J. A. Capobianco, *ACSNano*, 2010, **4**, 3254-3258.
10. C. D. S. Brites, B. Zhuang, M. L. Debasu, D. Ding, X. Qin, F. E. Maturi, W. W. Y. Lim, W. Soh, J. Rocha, Z. Yi, X. Liu and L. D. Carlos, *J Phys Chem Lett*, 2020, **11**, 6704-6711.
11. A. Lay, C. Siefe, S. Fischer, R. D. Mehlenbacher, F. Ke, W. L. Mao, A. P. Alivisatos, M. B. Goodman and J. A. Dionne, *Nano Lett.*, 2018, **18**, 4454-4459.
12. M. He, X. Pang, X. Liu, B. Jiang, Y. He, H. Snaith and Z. Lin,

Angew. Chem. Int. Ed. Engl., 2016, **128**, 4352-4356.

13. J. Day, S. Senthilarasu and T. K. Mallick, *Renew. Energy*, 2019, **132**, 186-205.
14. O. Laporte and W. F. Meggers, *J. Opt. Soc. Am.*, 1925, **11**, 464-564.
15. F. Auzel, *Chem. Rev.*, 2004, **104**, 139-173.
16. Q. Dou and Y. Zhang, *Langmuir*, 2011, **27**, 13236-13241.
17. J. Huang, J. Li, X. Zhang, W. Zhang, Z. Yu, B. Ling, X. Yang andY. Zhang, *Nano Lett.*, 2020, **20**, 5236-5242.
18. L. Lei, D. Chen, J. Xu, R. Zhang and Y. Wang, *Chem. Asian J.*,2014, **9**, 728-733.
19. T. Cheng, R. Marin, A. Skripka and F. Vetrone, *J. Am. Chem.Soc.*, 2018, **140**, 12890-12899.
20. X. Chen, D. Peng, Q. Ju and F. Wang, *Chem. Soc. Rev.*, 2015, **44**, 1318-1330.
21. D. Hudry, I. A. Howard, R. Popescu, D. Gerthsen and B. S.Richards, *Adv. Mater.*, 2019, **31**, e1900623.
22. D. Peng, Q. Ju, X. Chen, R. Ma, B. Chen, G. Bai, J. Hao, X. Qiao,X. Fan and F. Wang, *Chem. Mater.*, 2015, **27**, 3115-3120.
23. R. Marin, G. Sponchia, P. Riello, R. Sulcis and F. Enrichi, *J.Nanopart. Res.*, 2012, **14**, 886.
24. M. Back, E. Trave, R. Marin, N. Mazzucco, D. Cristofori and P.Riello, *J. Phys. Chem. C*, 2014, **118**, 30071-30078.
25. K. Trejgis and L. Marciniak, *Phys. Chem. Chem. Phys.*, 2018, **20**, 9574-9581.
26. M. Saboktakin, X. Ye, U. K. Chettiar, N. Engheta, C. B. Murrayand C. R. Kagan, *ACS Nano*, 2013, **7**, 7186-7192.
27. K. T. Lee, J. H. Park, S. J. Kwon, H. K. Kwon, J. Kyhm, K. W. Kwak, H. S. Jang, S. Y. Kim, J. S. Han, S. H. Lee, D. H. Shin, H. Ko, I. K. Han, B. K. Ju, S. H. Kwon and D. H. Ko, *Nano Lett.*, 2015, **15**, 2491-2497.

28. W. Park, D. Lu and S. Ahn, *Chem. Soc. Rev.*, 2015, **44**, 2940-2962.
29. A. Skripka, T. Cheng, C. M. S. Jones, J. Marques-Hueso, R.Marin and F. Vetrone, *Nanoscale*, 2020, **12**, 17545-17554.
30. D. Lu, S. K. Cho, S. Ahn, L. Brun, C. J. Summers and W. Park, *ACS Nano*, 2014, **8**, 7780-7792.
31. S. Rohani, M. Quintanilla, S. Tuccio, F. De Angelis, E. Cantelar, A. O. Govorov, L. Razzari and F. Vetrone, *Adv. Opt. Mater.*,2015, **3**, 1606-1613.
32. J. He, W. Zheng, F. Ligmajer, C. F. Chan, Z. Bao, K. L. Wong, X.Chen, J. Hao, J. Dai, S. F. Yu and D. Y. Lei, *Light Sci. Appl.*, 2017,**6**, e16217.
33. H. Li, Q. Deng, B. Liu, J. Yang and B. Wu, *RSC Adv.*, 2016, **6**, 13343-13348.
34. Z. Li, L. Wang, Z. Wang, X. Liu and Y. Xiong, *J. Phys. Chem. C*, 2011, **115**, 3291-3296.
35. P. Yuan, Y. H. Lee, M. K. Gnanasammandhan, Z. Guan, Y. Zhang and Q. H. Xu, *Nanoscale*, 2012, **4**, 5132-5137.
36. P. Kannan, F. Abdul Rahim, R. Chen, X. Teng, L. Huang, H. Sunand D. H. Kim, *ACS Appl. Mater. Interfaces*, 2013, **5**, 3508-3513.
37. P. Kannan, F. A. Rahim, X. Teng, R. Chen, H. Sun, L. Huang andD.-H. Kim, *RSC Adv.*, 2013, **3**, 7718-7721.
38. S. Fischer, D. Kumar, F. Hallermann, G. von Plessen and J. C. Goldschmidt, *Opt. Express*, 2016, **24**, A460-475.
39. Y. Xue, C. Ding, Y. Rong, Q. Ma, C. Pan, E. Wu, B. Wu and H. Zeng, *Small*, 2017, **13**, 1701155.
40. D. Mendez-Gonzalez, S. Melle, O. G. Calderon, M. Laurenti, E.Cabrera-Granado, A. Egatz-Gomez, E. Lopez-Cabarcos, J. Rubio-Retama and E. Diaz, *Nanoscale*, 2019, **11**, 13832- 13844.
41. Q. Zhan, X. Zhang, Y. Zhao, J. Liu and S. He, *Laser Photonics Rev.*, 2015, **9**, 479-487.
42. F. Kang, J. He, T. Sun, Z. Y. Bao, F. Wang and D. Y. Lei, *Adv. Funct. Mater.*, 2017, **27**, 1701842.
43. Y. Chen, K. Munechika and D. S. Ginger, *Nano Lett.*, 2007, **7**, 690-696.
44. D. M. Wu, A. Garcia-Etxarri, A. Salleo and J. A. Dionne, *J. Phys.Chem. Lett.*, 2014, **5**, 4020-4031.
45. A. Das, C. Mao, S. Cho, K. Kim and W. Park, *Nat. Commun.*, 2018, **9**, 4828.
46. M. Kanehara, H. Koike, T. Yoshinaga and T. Teranishi, *J. Am. Chem. Soc.*, 2009, **131**, 17736-17737.
47. J. Li, W. Zhang, C. Lu, Z. Lou and B. Li, *Nanoscale Horiz.*, 2019, **4**, 999-1005.
48. D. Zhou, D. Liu, W. Xu, Z. Yin, X. Chen, P. Zhou, S. Cui, Z. Chenand H. Song, *ACS Nano*, 2016, **10**, 5169-5179.
49. T. M. Mattox, A. Agrawal and D. J. Milliron, *Chem. Mater.*,2015, **27**, 6620-6624.
50. Y. Ma, L. Zhang, L. Wang, L. Wang and H. Chen, *Anal.Methods*, 2017, **9**, 2977-2982.
51. H. Zhang, Y. Li, I. A. Ivanov, Y. Qu, Y. Huang and X. Duan, *Angew. Chem. Int. Ed. Engl.*, 2010, **49**, 2865-2868.
52. Y. Qin, Z. Dong, D. Zhou, Y. Yang, X. Xu and J. Qiu, *Opt. Mater.Express*, 2016, **6**, 1942-1955.
53. H. Xing, W. Bu, S. Zhang, X. Zheng, M. Li, F. Chen, Q. He, L. Zhou, W. Peng, Y. Hua and J. Shi, *Biomaterials*, 2012, **33**, 1079-1089.
54. T. Jiang, J. Li, W. Qin and J. Zhou, *J. Lumin.*, 2014, **156**, 164- 169.
55. M. Rai, S. K. Singh, A. K. Singh, R. Prasad, B. Koch, K. Mishra and S. B. Rai, *ACS Appl. Mater. Interfaces*, 2015, **7**, 15339-15350.
56. S. Liu, G. Chen, T. Y. Ohulchanskyy, M. T. Swihart and P. N. Prasad, *Theranostics*, 2013, **3**, 275-281.
57. S. Wu, N. Duan, Z. Shi, C. Fang and Z. Wang, *Talanta*, 2014, **128**, 327-336.
58. M. Runowski, *J. Lumin.*, 2017, **186**, 199-204.
59. M. Sun, L. Xu, W. Ma, X. Wu, H. Kuang, L. Wang and C. Xu, *Adv. Mater.*, 2016, **28**, 898-904.
60. C. Zhang and J. Y. Lee, *J. Phys. Chem. C*, 2013, **117**, 15253-15259.
61. L. Sudheendra, V. Ortalan, S. Dey, N. D. Browning and I. M.Kennedy, *Chem. Mater.*, 2011, **23**, 2987-2993.
62. A. Priyam, N. M. Idris and Y. Zhang, *J. Mater. Chem.*, 2012, **22**,960-965.
63. Y. Song, G. Liu, J. Wang, X. Dong and W. Yu, *Phys. Chem.Chem. Phys.*, 2014, **16**, 15139-15145.
64. D. Yin, C. Wang, J. Ouyang, X. Zhang, Z. Jiao, Y. Feng, K. Song, B. Liu, X. Cao, L. Zhang, Y. Han and M. Wu, *ACS Appl. Mater.Interfaces*, 2014, **6**, 18480-18488.
65. F. Zhang, G. B. Braun, Y. Shi, Y. Zhang, X. Sun, N. O. Reich, D.Zhao and G. Stucky, *J. Am. Chem. Soc.*, 2010, **132**, 2850-2851.
66. W. Ge, X. R. Zhang, M. Liu, Z. W. Lei, R. J. Knize and Y. Lu,

Theranostics, 2013, **3**, 282-288.

67. Y. Zhang, J. Wang, F. Nan and Q.-Q. Wang, *RSC Adv.*, 2018, **8**,20056-20060.
68. B. A. R. Aiken, W. P. Hsu and E. Matijevic, *J. Am. Ceram. Soc.*,1988, **71**, 845-853.
69. Y. Huang, F. Rosei and F. Vetrone, *Nanoscale*, 2015, **7**, 5178-5185.
70. C. Wang, C. Xu, L. Xu, C. Sun, D. Yang, J. Xu, F. He, S. Gai andP. Yang, *J. Mater. Chem. B*, 2018, **6**, 2597-2607.
71. C. Wang, L. Xu, J. Xu, D. Yang, B. Liu, S. Gai, F. He and P. Yang, *Dalton. Trans.*, 2017, **46**, 12147-12157.
72. F. Xu, H. Gao, J. Liang, S. Jin, J. Zhao, Y. Liu, H. Zhang, Z. Zhangand Y. Mao, *Ceram. Int.*, 2019, **45**, 21557-21563.
73. N. J. Greybush, M. Saboktakin, X. Ye, C. Della Giovampaola, S. J. Oh, N. E. Berry, N. Engheta, C. B. Murray and C. R. Kagan, *ACS Nano*, 2014, **8**, 9482-9491.
74. T. Hinamoto, H. Takashina, H. Sugimoto and M. Fujii, *J. Phys.Chem. C*, 2017, **121**, 8077-8083.
75. T. Hinamoto, T. Higashiura, H. Sugimoto and M. Fujii, *J. Phys.Chem. C*, 2019, **123**, 25809-25815.
76. X. Wang, R. R. Valiev, T. Y. Ohulchanskyy, H. Agren, C. Yangand G. Chen, *Chem. Soc. Rev.*, 2017, **46**, 4150-4167.
77. D. J. Garfield, N. J. Borys, S. M. Hamed, N. A. Torquato, C. A.Tajon, B. Tian, B. Shevitski, E. S. Barnard, Y. D. Suh, S. Aloni, J. B. Neaton, E. M. Chan, B. E. Cohen and P. J. Schuck, *Nat.Photonics*, 2018, **12**, 402-407.
78. J. Lee, B. Yoo, H. Lee, G. D. Cha, H. S. Lee, Y. Cho, S. Y. Kim, H.Seo, W. Lee, D. Son, M. Kang, H. M. Kim, Y. I. Park, T. Hyeon and D. H. Kim, *Adv. Mater.*, 2017, **29**, 1603169.
79. Q. Liu, X. Zou, Y. Shi, B. Shen, C. Cao, S. Cheng, W. Feng and F. Li, *Nanoscale*, 2018, **10**, 12573-12581.
80. X. Zou, M. Xu, W. Yuan, Q. Wang, Y. Shi, W. Feng and F. Li, *Chem. Commun. (Camb.)*, 2016, **52**, 13389-13392.
81. D. L. Dexter, *J. Chem. Phys.*, 1953, **21**, 836-850.
82. Z. Q. You, C. P. Hsu and G. R. Fleming, *J. Chem. Phys.*, 2006, **124**, 044506.
83. S. I. Weissman, *J. Chem. Phys.*, 1942, **10**, 214-217.

84. J. P. Leonard, C. B. Nolan, F. Stomeo and T. Gunnlaugsson, in *Photochemistry and Photophysics of Coordination Compounds II*, 2007, Chapter 142, pp. 1-43, Springer-Verlag Berlin Heidelberg.
85. J. Zhang, C. M. Shade, D. A. Chengelis and S. Petoud, *J. Am. Chem. Soc.*, 2007, **129**, 14834-14835.
86. L. J. Charbonnière, J.-L. Rehspringer, R. Ziessel and Y. Zimmermann, *New J. Chem.*, 2008, **32**, 1055–1059.
87. W. Zou, C. Visser, J. A. Maduro, M. S. Pshenichnikov and J. C.Hummelen, *Nat. Photonics*, 2012, **6**, 560-564.
88. G. Chen, J. Damasco, H. Qiu, W. Shao, T. Y. Ohulchanskyy, R. R. Valiev, X. Wu, G. Han, Y. Wang, C. Yang, H. Agren and P. N.Prasad, *Nano Lett.*, 2015, **15**, 7400-7407.
89. C. Hazra, S. Ullah, Y. E. Serge Correales, L. G. Caetano and S. J. L. Ribeiro, *J. Mater. Chem. C*, 2018, **6**, 4777-4785.
90. S. Hao, Y. Shang, D. Li, H. Agren, C. Yang and G. Chen, *Nanoscale*, 2017, **9**, 6711-6715.
91. W. Shao, G. Chen, A. Kuzmin, H. L. Kutscher, A. Pliss, T. Y. Ohulchanskyy and P. N. Prasad, *J. Am. Chem. Soc.*, 2016, **138**, 16192-16195.
92. U. Resch-Genger, M. Grabolle, S. Cavaliere-Jaricot, R. Nitschke and T. Nann, *Nat. Methods*, 2008, **5**, 763-775.
93. W. Zhang, T. Chen, L. Su, X. Ge, X. Chen, J. Song and H. Yang, *Anal. Chem.*, 2020, **92**, 6094-6102.
94. D. Song, S. Chi, X. Li, C. Wang, Z. Li and Z. Liu, *ACS Appl. Mater.Interfaces*, 2019, **11**, 41100-41108.
95. S. E. Creutz, R. Fainblat, Y. Kim, M. C. De Siena and D. R. Gamelin, *J. Am. Chem. Soc*,. 2017, **139**, 11814-11824.
96. T. J. Milstein, D. M. Kroupa and D. R. Gamelin, *Nano Lett.*, 2018, **18**, 3792-3799.
97. R. Marin, L. Labrador-Paéz, A. Skripka, P. Haro-González, A. Benayas, P. Canton, D. Jaque and F. Vetrone, *ACS Photonics*, 2018, **5**, 2261-2270.
98. S. Bhuckory, E. Hemmer, Y.-T. Wu, A. Yahia-Ammar, F. Vetrone and N. Hildebrandt, *Eur. J. Inorg. Chem.*, 2017, **2017**, 5186-5195.
99. R. Marin and D. Jaque, **under review**.
100. W. J. Mir, T. Sheikh, H. Arfin, Z. Xia and A. Nag, *NPG Asia Mater.*, 2020, **12**, 9.
101. Y. Zhao, F. T. Rabouw, T. van Puffelen, C. A. van Walree, D. R.Gamelin, C. de Mello Donega and A. Meijerink, *J. Am. Chem.Soc.*, 2014, **136**, 16533-16543.
102. M. Makkar, A. Saha, S. Khalid and R. Viswanatha, *J. Phys. Chem. Lett.*, 2019, **10**, 1992-1998.
103. L. De Trizio and L. Manna, *Chem. Rev.*, 2016, **116**, 10852- 10887.
104. V. A. Vlaskin, C. J. Barrows, C. S. Erickson and D. R. Gamelin, *J. Am. Chem. Soc.*, 2013, **135**, 14380-14389.
105. J. Planelles-Aragó, E. Cordoncillo, R. A. S. Ferreira, L. D. Carlosand P. Escribano, *J. Mater. Chem.*, 2011, **21**, 1162-1170.
106. D. A. Chengelis, A. M. Yingling, P. D. Badger, C. M. Shade andS. Petoud, *J. Am. Chem. Soc.*, 2005, **127**, 16752-16753.
107. R. Martin-Rodriguez, R. Geitenbeek and A. Meijerink, *J. Am.Chem. Soc.*, 2013, **135**, 13668-13671.
108. P. Mukherjee, C. M. Shade, A. M. Yingling, D. N. Lamont, D. H. Waldeck and S. Petoud, *J. Phys. Chem. A*, 2011, **115**, 4031-4041.
109. A. A. Bol, R. van Beek and A. Meijerink, *Chem. Mater.*, 2002, **14**, 1121-1126.
110. V. Kumar, O. M. Ntwaeaborwa, T. Soga, V. Dutta and H. C.Swart, *ACS Photonics*, 2017, **4**, 2613-2637.
111. V. Štengl, S. Bakardjieva and N. Murafa, *Mater. Chem. Phys.*,2009, **114**, 217-226.
112. Q. Xiao, Y. Liu, L. Liu, R. Li, W. Luo and X. Chen, *J. Phys. Chem.C*, 2010, **114**, 9314-9321.
113. T. Wang, A. Layek, I. D. Hosein, V. Chirmanov and P. V.Radovanovic, *J. Mater. Chem. C*, 2014, **2**, 3212-3222.
114. M. Zhang, W. Zheng, Y. Liu, P. Huang, Z. Gong, J. Wei, Y. Gao, S. Zhou, X. Li and X. Chen, *Angew. Chem. Int. Ed. Engl.*, 2019, **58**, 9556-9560.
115. D. C. Rodríguez Burbano, E. M. Rodríguez, P. Dorenbos, M. Bettinelli and J. A. Capobianco, *J. Mater. Chem. C*, 2014, **2**, 228-231.
116. J. Wang, Y. Zhu, C. A. Grimes and Q. Cai, *Nanoscale*, 2019, **11**,12497-12501.
117. X. Qin, X. Liu, W. Huang, M. Bettinelli and X. Liu, *Chem. Rev.*,2017, **117**, 4488-4527.
118. X. Li, S. Duan, H. Liu, G. Chen, Y. Luo and H. Ågren, *J. Phys. Chem. Lett.*, 2019, **10**, 487-492.
119. J. Kang and L. W. Wang, *J. Phys. Chem. Lett.*, 2017, **8**, 489- 493.
120. J.-P. Ma, Y.-M. Chen, L.-M. Zhang, S.-Q. Guo, J.-D. Liu, H. Li, B.-J. Ye, Z.-Y. Li, Y. Zhou, B.-B. Zhang, O. M. Bakr, J.-Y. Zhang and H.-T. Sun, *J. Mater. Chem. C*, 2019, **7**, 3037-3048.
121. G. Pan, X. Bai, D. Yang, X. Chen, P. Jing, S. Qu, L. Zhang, D. Zhou, J. Zhu, W. Xu, B. Dong and H. Song, *Nano Lett.*, 2017, **17**, 8005-8011.

122. D. Zhou, R. Sun, W. Xu, N. Ding, D. Li, X. Chen, G. Pan, X. Baiand H. Song, *Nano Lett.*, 2019, **19**, 6904-6913.
123. D. Zhou, D. Liu, G. Pan, X. Chen, D. Li, W. Xu, X. Bai and H.Song, *Adv. Mater.*, 2017, **29**.
124. G. Pan, X. Bai, W. Xu, X. Chen, D. Zhou, J. Zhu, H. Shao, Y. Zhai, B. Dong, L. Xu and H. Song, *ACS Appl. Mater. Interfaces*, 2018, **10**, 39040-39048.
125. Z. Wang, Z. Shi, T. Li, Y. Chen and W. Huang, *Angew. Chem.Int. Ed. Engl.*, 2017, **56**, 1190-1212.
126. L. Wang, H. Zhou, J. Hu, B. Huang, M. Sun, B. Dong, G. Zheng, Y. Huang, Y. Chen, L. Li, Z. Xu, N. Li, Z. Liu, Q. Chen, L. D. Sun and C. H. Yan, *Science*, 2019, **363**, 265-270.
127. W. Lee, S. Hong and S. Kim, *J. Phys. Chem. C*, 2019, **123**, 2665-2672.
128. N. Chen, T. Cai, W. Li, K. Hills-Kimball, H. Yang, M. Que, Y. Nagaoka, Z. Liu, D. Yang, A. Dong, C. Y. Xu, R. Zia and O. Chen, *ACS Appl. Mater. Interfaces*, 2019, **11**, 16855-16863.
129. N. Ding, D. Zhou, G. Pan, W. Xu, X. Chen, D. Li, X. Zhang, J. Zhu, Y. Ji and H. Song, *ACS Sust. Chem. Engin.*, 2019, **7**, 8397-8404.
130. Y. Zhu, J. Zhu, H. Song, J. Huang, Z. Lu and G. Pan, *J. Rare Earths*, 2020, DOI: 10.1016/j.jre.2020.06.007.
131. O. M. ten Kate, H. T. Hintzen, P. Dorenbos and E. van der Kolk, *J. Mater. Chem.*, 2011, **21**, 18289-18294.
132. M. A. Klik, T. Gregorkiewicz, I. V. Bradley and J. P. Wells, *Phys.Rev. Lett.*, 2002, **89**, 227401.
133. P. Dorenbos, *J. Phys. Conde. Matter*, 2003, **15**, 8417-8434.
134. P. Dorenbos, *Opt. Mater.*, 2017, **69**, 8-22.
135. J. K. Swabeck, S. Fischer, N. D. Bronstein and A. P. Alivisatos, *J. Am. Chem. Soc.*, 2018, **140**, 9120-9126.
136. F. Wang, S. Cheng, Z. Bao and J. Wang, *Angew. Chem. Int. Ed.Engl.*, 2013, **52**, 10344-10348.
137. L. Labrador-Paez, E. C. Ximendes, P. Rodriguez-Sevilla, D. H. Ortgies, U. Rocha, C. Jacinto, E. Martin Rodriguez, P. Haro-Gonzalez and D. Jaque, *Nanoscale*, 2018, **10**, 12935-12956.
138. Y. Fan, L. Liu and F. Zhang, *Nano Today*, 2019, **25**, 68-84.